HIGHWAY RESEARCH RECORD

Number 101

Frost Action and Insulation Against Subgrade Freezing

4 Reports

Presented at the
44th ANNUAL MEETING
January 11-15, 1965

SUBJECT CLASSIFICATION
62 Foundations (Soils)
64 Soil Science
25 Pavement Design

HIGHWAY RESEARCH BOARD
of the
Division of Engineering and Industrial Research
National Academy of Sciences—National Research Council
Washington, D. C.
1965

Department of Soils, Geology and Foundations

Eldon J. Yoder, Chairman
Joint Highway Research Project
Purdue University, Lafayette, Indiana

DIVISION C

O. L. Lund, Chairman
Assistant Engineer of Materials and Tests, Highway Testing Laboratory
Nebraska Department of Roads, Lincoln

COMMITTEE ON FROST ACTION

(As of December 31, 1964)

L. F. Erickson, Chairman
Research Engineer
Idaho Department of Highways, Boise

C. B. Crawford, Soil Mechanics Section, Division of Building Research, National Research Council, Ottawa, Canada
Hamilton Gray, Chairman, Department of Civil Engineering, Ohio State University, Columbus
L. E. Gregg, L. E. Gregg and Associates, Consulting Engineers, Lexington, Kentucky
W. M. Haas, Michigan Technological University, Houghton
Frank B. Hennion, Assistant Chief, Civil Engineering Branch, Engineering Division, Military Construction, Office, Chief of Engineers, Department of the Army, Washington, D. C.
Alfreds R. Jumikis, Professor of Civil Engineering, College of Engineering, Rutgers, The State University, New Brunswick, New Jersey
Miles S. Kersten, Professor of Civil Engineering, University of Minnesota, Minneapolis
R. I. Kingham, Research Engineer, Department of Highways, Downsview, Ontario, Canada
O. L. Lund, Assistant Materials and Testing Engineer, Highway Testing Laboratory, Nebraska Department of Roads, Lincoln
A. E. Matthews, Engineer of Soils, Office of Testing and Research, Michigan State Highway Department, Lansing
George W. McAlpin, Deputy Chief Engineer (Research), Technical Services Subdivision, New York State Department of Public Works, Albany
Eugene B. McDonald, Materials Engineer, South Dakota Department of Highways, Pierre
Paul S. Otis, Materials and Research Engineer, New Hampshire Department of Public Works and Highways, Concord
R. G. Packard, Portland Cement Association, Chicago, Illinois
C. K. Preus, Materials and Research Engineer, Minnesota Department of Highways, St. Paul
James R. Schuyler, State Highway Engineer, New Jersey State Highway Department, Trenton
Willis H. Taylor, Jr., Bituminous Construction Engineer, Louisiana Department of Highways, Baton Rouge
K. B. Woods, Head, School of Civil Engineering and Director, Joint Highway Research Project, Purdue University, Lafayette, Indiana

Foreword

Freezing may adversely affect subgrades and base courses by causing non-uniform heaving during the freezing period and reduction in strength during the thawing period. For many years, researchers have sought to understand the underlying phenomena that cause these changes, but because adequate understanding of fundamentals often develops slowly, these same researchers also have resorted to very practical pursuits in an attempt to cut down the detrimental effects.

This Record illustrates well this two-way attack on the problem. Two of the papers report the results of studies that markedly broaden out understanding of the basic nature of what takes place during the freezing and thawing periods.

In the past, attempts have been made to measure the degree of frost damage susceptibility of soils in terms of rate of heaving. Hoekstra, Chamberlain and Frate show the possibilities of assessing the frost susceptibility in terms of the heave pressures developed by freezing a saturated soil in an open system (where the soil below the freezing zone has access to free water). The results are encouraging and certainly warrant broader studies of this aspect of soil freezing.

When detrimental soil freezing occurs, layers on "lenses" of ice occur. This segregates the water that was previously distributed through the soil. The strength (bearing capacity) of the soil before freezing is dependent upon the friction and/or cohesion developed through interparticle contact. When water fills the pores and a load is placed on the soil, the effective interparticle contact is reduced, thus reducing strength. Yao and Broms investigate the excess pore pressures that occur during thawing within a subgrade. Their studies show that the excess pore pressures decrease rapidly in a zone close to a pervious layer.

Two other papers report on investigations concerning the use of "foamed plastic" insulating layers placed under the pavement and above the subgrade in attempts to limit the depth of soil freezing. Both the Young experiment, made near Winnipeg, Manitoba, and the Oosterbaan and Leonards study made at Purdue University, show that the use of the insulating layers either completely prevented subgrade freezing or permitted only minor subgrade freezing depending upon the overlying pavement thickness and the thickness of the insulation.

The papers contained in this Record are excellent examples of research studies that add much to our knowledge of the nature of soil freezing and thawing and how to prevent detrimental frost action.

Highway Research Correlation Service

HIGHWAY RESEARCH BOARD of the
National Academy of Sciences—National Research Council
2101 Constitution, Washington, D.C.

HIGHWAY RESEARCH RECORD 101

FROST ACTION AND INSULATION AGAINST SUBGRADE FREEZING

This 57-page book contains four papers presented at the 44th Annual Meeting of the Highway Research Board, as follows:

"Experimental Foamed Plastic Base Course," by Fred D. Young.

"Use of Insulating Layer to Attenuate Frost Action in Highway Pavements," by M. D. Oosterbaan and G. A. Leonards.

"Frost-Heaving Pressures," by P. Hoekstra, E. Chamberlain, and T. Frate.

"Excess Pore Pressures Which Develop During Thawing of Frozen Fine-Grained Subgrade Soils," by Leslie Y. C. Yao and Bengt B. Broms.

Price $1.20 December 1965

Contents

Experimental Foamed Plastic Base Course

FRED D. YOUNG, Materials and Research Engineer, Manitoba Highways Branch

Procedures implemented to install foamed plastic on a clay subgrade near Winnipeg are described. The foam was a rigid polystyrene which was placed on the subgrade and covered with 12 in. of gravel base and a 4-in. bituminous surface. Information obtained by means of thermocouples indicated that thicknesses of foam of 2 in. reduced frost penetration to a few inches in the subgrade and 3¼ in. of foam essentially prevented frost penetration. The control section showed that the rigorous climate which generally experiences 3,500 degree-days of frost resulted in frost penetration of 7 ft when foamed plastic is not used.

•BECAUSE OF the development of the plastics industry and the many forms of plastics which were becoming available, a keen interest has been taken by the Manitoba Highways Branch in the uses of these materials. Interest in plastics as a base course replacement was caused by the possibility of shortages of gravel supplies in some areas and by road development in muskeg areas. The latter was a factor which led to discussions pertaining to the floating of roadbeds on lightweight foamed plastic bases over undisturbed muskeg. The economics of this application, however, were not attractive enough to create interest in an experiment.

Because gravel shortages could increase the cost of standard base construction and increased sales of foamed plastic could reduce their cost, attention was turned to replacement of gravel by foamed plastic in a standard highway section. Further discussions within the Materials and Research Section and with representatives of Dow Chemical of Canada Ltd. created much interest in the possible side benefit in controlling the spring thawing of the subgrade. The prevention of thawing from the top of the subgrade would allow the thaw to occur from the bottom of the frozen layer, thus allowing ice lens water to escape into the subgrade rather than to be trapped above the frozen layer creating a weak structure. The further possibility that frost penetration could be reduced or eliminated made a trial project extremely attractive.

Departmental approval was obtained for a trial, arrangements were made for the supply of foamed plastic by the Dow Chemical Co., and a location was chosen in the fall of 1962.

PROJECT LOCATION

The site selected for this trial is a 300-ft section of the Trans-Canada Highway approximately 11 mi east of Winnipeg. This portion of the northbound 2 lanes of the 4-lane divided highway is located immediately west of the end of concrete pavement and lies in a bituminous-surfaced section to be removed on construction of the Winnipeg Floodway. The site was nearly ideal in that the subgrade was well constructed, a nearby bituminous paving project could provide equipment and materials, and the highway carries relatively heavy traffic. In addition, it is located near Winnipeg for easy access by department personnel.

Winnipeg is approximately 60 mi north of the Manitoba-Minnesota border and experiences 3,500 degree-days of frost. Temperatures range from 100 to -40 F and

Paper sponsored by Committee on Frost Action.

depth of frost penetration under a pavement is generally from 5 to 7 ft. Precipitation is about 20 in. annually.

The Trans-Canada Highway in this location does not carry spring load restrictions and, therefore, the test section would be subject to fairly heavy loads throughout the year.

MATERIALS

The subgrade was constructed in a rural cross-section and consisted of a fat, A-7-5 (20) clay. This clay, commonly referred to as Red River Gumbo, exhibited a standard AASHO density of 97 pcf and an optimum moisture content of 25 percent. The classification tests yielded a liquid limit of 66 percent, and a plasticity index of 43. The soil consisted of 4 percent fine sand (passing a No. 40 sieve and retained on a No. 200), 16 percent silt (passing a No. 200 sieve but larger than 5μ) and 80 percent clay (smaller than 5μ). Results of density tests taken on the subgrade are given in Table 1.

Since the test area was only 300 ft in length subsectioned in three 100-ft lengths and each section had a different grade elevation requirement, it was difficult to provide a smooth surface on which to lay the foam plastic. To facilitate leveling, a thin layer of sand, approximately ½ in. in depth, was spread over the soil grade.

The foamed plastic, Styrofoam, was a continuously extruded, rigid polystyrene foam. The material was supplied in 4- by 8-ft sheets in thicknesses of 1½, 1¾ and 2 in. The sheets were held in place by wooden skewers. An asphalt emulsion was also supplied for painting joints between the sheets in an effort to seal them.

The gravel base course provided had the gradation given in Table 2. The gravel base was placed in a depth of 12 in. and compacted by a vibratory compactor to densities found to be 135.6 pcf at 3.0 percent moisture and 137.5 pcf at 2.7 percent moisture.

The bituminous material was placed in two lifts of 2 in. each. The first lift, with an asphalt content of 4.0 percent, was placed on the gravel base which had been primed the previous day with an MC-0 at a rate of 0.25 gal/sq yd. The second lift had an asphalt content of 5.0 percent and was placed after the first lift had received a fog coat of 0.05 gal/sq yd. Both lifts were bound by 150/200 penetration asphalt cement and were laid with a Barber-Greene Model 879 paver. Rolling was accomplished by an 8-ton Huber-Worco steel roller for breakdown and finishing and a Rosco rubber tire roller with a gross weight of 27,000 lb and tire pressure of 85 psi for intermediate rolling.

The analysis of four samples taken from the road is given in Table 3.

INSTRUMENTATION

The test area was thoroughly instrumented with thermocouples at various depths and locations to measure pavement and soil temperatures throughout the year.

TABLE 1

RESULTS OF DENSITY TESTS ON SUBGRADE

Dry Density (pcf)	Moisture Content (%)
92.0	17.7
83.8	22.6
100.0	15.0
95.5	16.8
84.0	24.1

TABLE 2

Sieve Size	% Passing	
1 in.	100	100
¾ in.	97	90
½ in.	80	82
⅜ in.	73	75
No. 4	54	63
No. 10	41	51
No. 40	19	22
No. 80	12	14
No. 100	11	12
No. 200	9	10

TABLE 3
ANALYSES OF BITUMINOUS MIX

Analysis	Sample			
	1	2	3	4
Station	441	441	438	440
Lift	1st	1st	2nd	2nd
Type of material	Base	Base	Mat.	Mat.
Residual asphalt content (%)	3.9	4.6	5.0	5.0
Marshall stability at 140 F (lb)	836	1,274	1,321	1,335
Marshall flow (0.01 in.)	13	13	11	13
Marshall density (pcf)	143.7	147.9	147.7	148.1
Aggregate density (pcf)	138.3	141.4	140.7	141.0
Aggregate volume (%)	83.6	85.5	85.0	85.2
Asphalt volume (%)	8.7	10.4	11.2	11.4
Volume of voids (%):				
In mix	7.7	4.1	3.8	3.4
In aggregate	16.4	14.5	15.0	14.8
Voids filled with asphalt (%)	53.0	71.7	74.7	77.0
Percent passing sieve:				
3/4 in.	100	100	100	100
5/8 in.	98	97	95	99
3/8 in.	75	74	80	81
No. 4	60	61	66	63
No. 10	51	51	53	51
No. 40	16	16	17	17
No. 200	4.6	5.3	6.1	6.1

Thermocouple equipment was supplied by Thermo-Electric (Canada) Ltd. Thermocouples were made by soldering the ends of 24-gage copper-constantan wire and coating them with Glyptal. Sets of these were then taped to 1- by 2-in. sticks and placed in previously augered holes. All wires were carried to the edge of the subgrade through plastic tubing. The resulting cables were spliced into coaxial cable at junction boxes and then connected to jack panels in the instrument building.

Reading of the temperature at each thermocouple was accomplished by plugging the male jack, connected to a direct-reading Rubicon No. 273 potentiometer, into the appropriate female connector on the jack panels. This method produced quick readings with a minimum effort.

A recording hygro-thermograph was mounted on the roof of the building to record humidity and air temperature.

CONSTRUCTION

The subgrade was shaped and compacted so that each section would have the same final cross-section and elevation. This was the most difficult portion of the work as

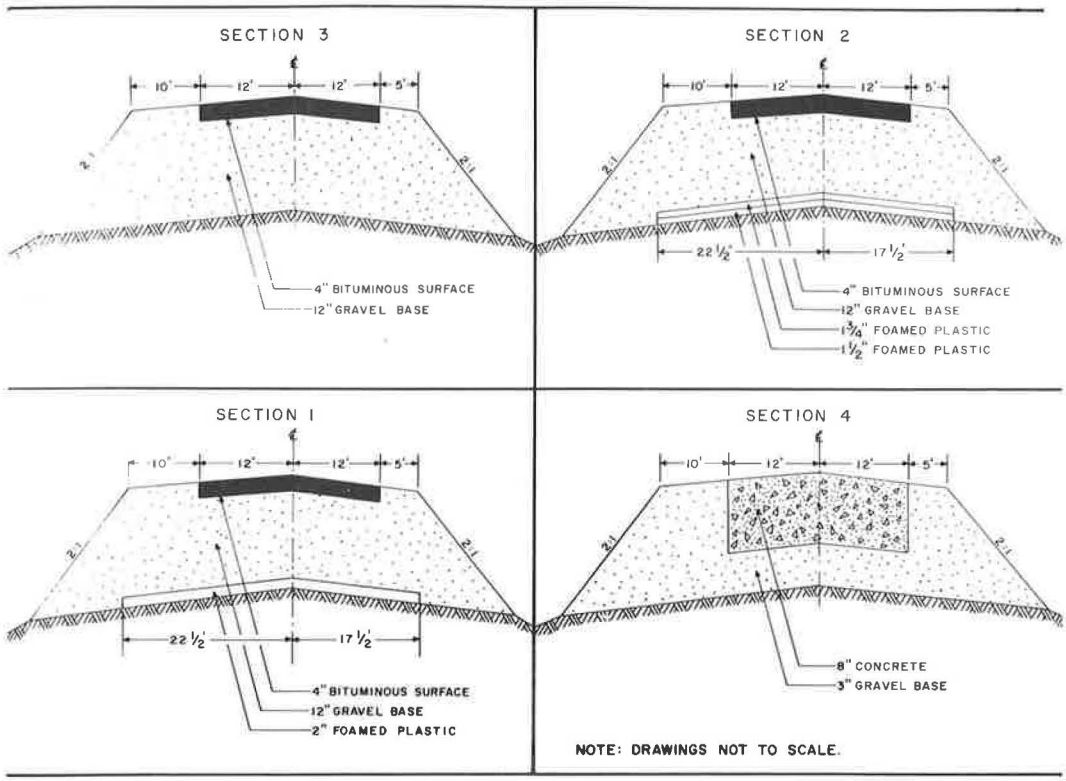

Figure 1. Cross-sections of test sections.

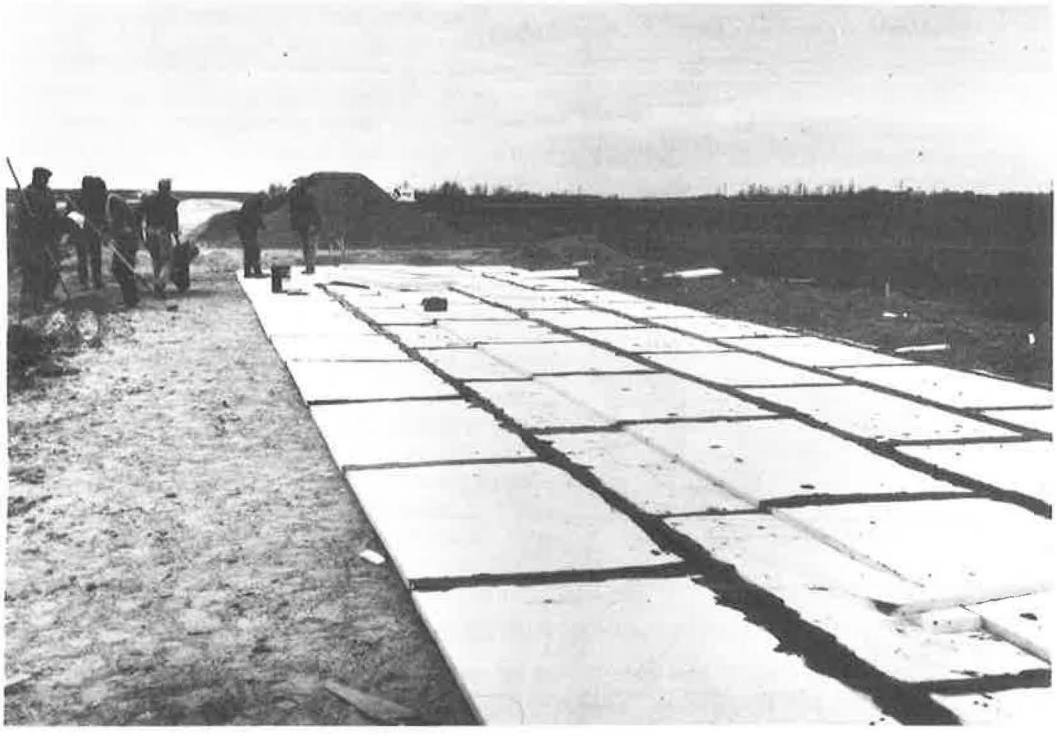

Figure 2. Partially completed section 2 showing two layers of foam plastic.

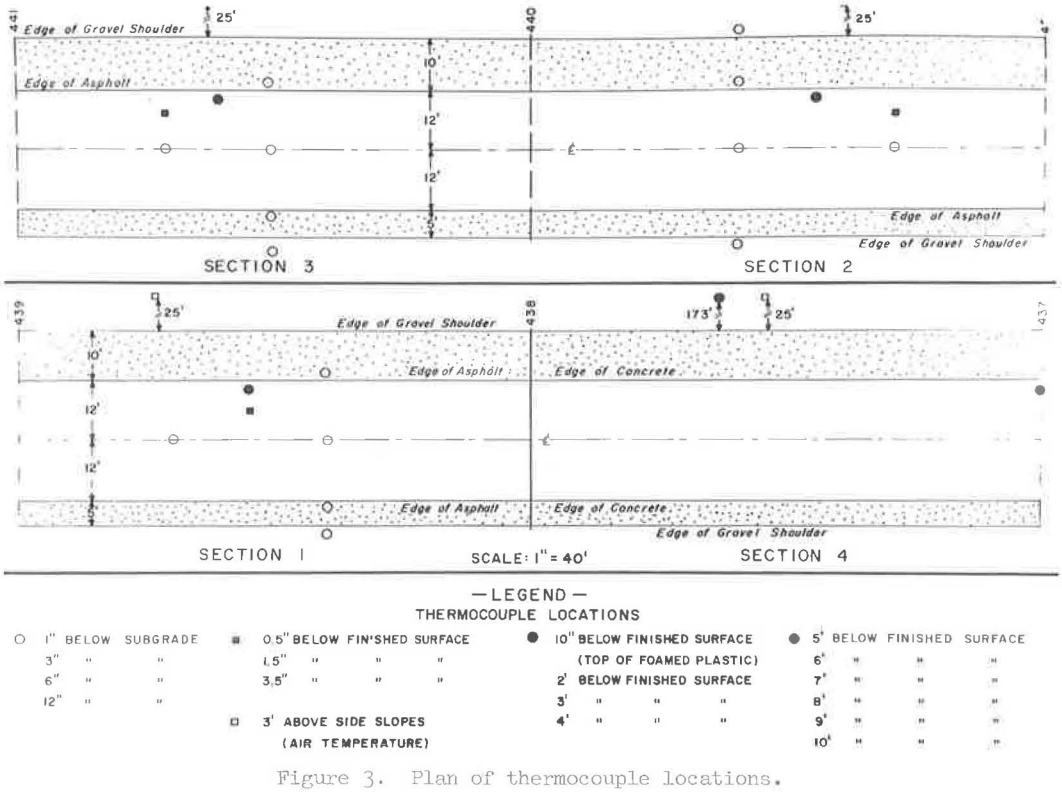

Figure 3. Plan of thermocouple locations.

Figure 4. Wedges of foam plastic being placed in gaps between sheets; machine placing base course on foam plastic.

the sections were only 100 ft long, which hardly allowed the motor grader and packers sufficient room to maneuver.

TABLE 4

BENKELMAN BEAM DEFLECTIONS ON FOAMED PLASTIC TEST SECTION

Date	Pavement Temperature (°F)	Deflections		
		Sect. 1	Sect. 2	Sect. 3
10/22/62	48	52	60	54
10/30/62	49	40	50	42
3/27/63	52	42	44	20
4/ 6/63	66	50	62	44
4/15/63	80	90	90	74
4/24/63	60	68	68	50
4/26/63	68	100	92	86
5/ 1/63	74	114	96	86
5/ 6/63	75	84	78	70
5/10/63	74	76	80	70
5/15/63	84	102	108	100
5/23/63	80	84	78	84
5/28/63	60	76	70	68
6/14/63	70	88	70	70
6/25/63	72	72	70	76
8/17/63	81	54	54	44
4/ 1/64	54	10	12	4
4/16/64	78	32	54	42
4/20/64	38	32	56	34
4/29/64	54	40	44	32
5/ 1/64	62	60	58	56
5/ 8/64	68	64	54	50
5/16/64	54	60	52	50
5/21/64	84	80	68	60
5/25/64	84	78	66	70
5/26/64	74	80	66	70
5/29/64	62	66	58	64
6/ 1/64	52	58	48	48
6/ 5/64	92	80	56	54
6/12/64	68	68	72	68
6/22/64	77	76	74	64

Following the fine-grading with $\frac{1}{2}$ in. of sand, work commenced on the placement of the foam plastic. The cross-sections for the project are shown in Figure 1. Section 1 received one layer of 2-in. by 4-ft by 8-ft foamed plastic sheets placed so as to reduce the continuity of the joints. The sheets were pegged into place by wooden skewers and the joints were painted with an asphalt emulsion. The difference in shoulder width is due to the divided highway median design in this area. Section 2 received one layer of $1\frac{1}{2}$-in. and one of $1\frac{3}{4}$-in. thick foam. Again the joints were staggered on each layer as well as from one layer to the next (Fig. 2). Section 3, the control section, received the same base, pavement, and instrumentation as sections 1 and 2, but was not insulated with foamed plastic.

The standard concrete pavement at the east end, adjacent to test section 1 is also shown in Figure 1.

The plan of thermocouple location is illustrated in Figure 3. The coded location points indicate similar installations. There are thermocouples in the adjacent field, the air at the shoulder, the subgrade, the base course and the bituminous pavement.

The base course was placed as soon as possible to help hold the plastic in place. A crawler tractor with a front end bucket was used to place the base gravel (Fig. 4). The base was dumped ahead of the machine to provide a ramp. When the initial ramp, about 8 to 12 in. thick and 10 to 20 ft wide, had been built along the length of the project, trucks were able to carry the gravel over the foamed plastic without damaging it.

The loader then loaded the trucks from the stockpile, the trucks deposited it, and a motor grader did the spreading. A depth of 12 in. of gravel base was used.

A vibratory compactor was used to attain density and the completed base was primed. The following day the two lifts of bituminous material were placed and compacted.

TEST RESULTS

Benkelman beam rebound measurements are taken throughout the spring, summer and fall. The results of these tests are given in Table 4.

Temperature measurements are taken periodically, more frequently during times of extreme temperature change such as spring and fall. Of the hundred of readings taken, only the more important ones are plotted in Figures 5 to 9.

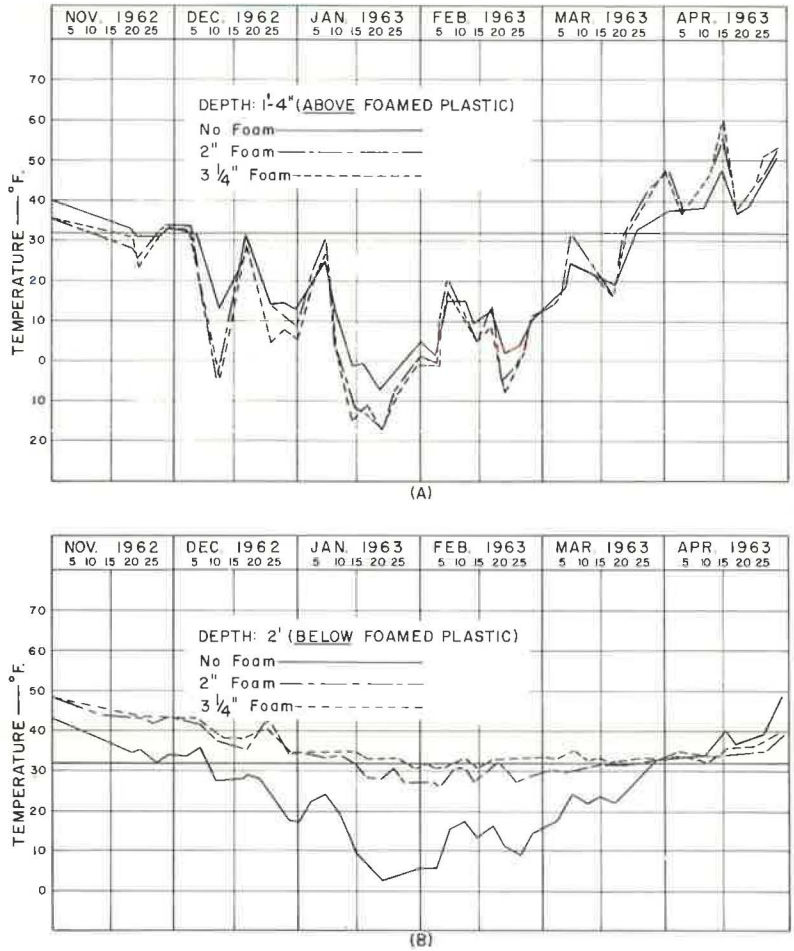

Figure 5. Variation in temperature above and below foamed plastic with time of year.

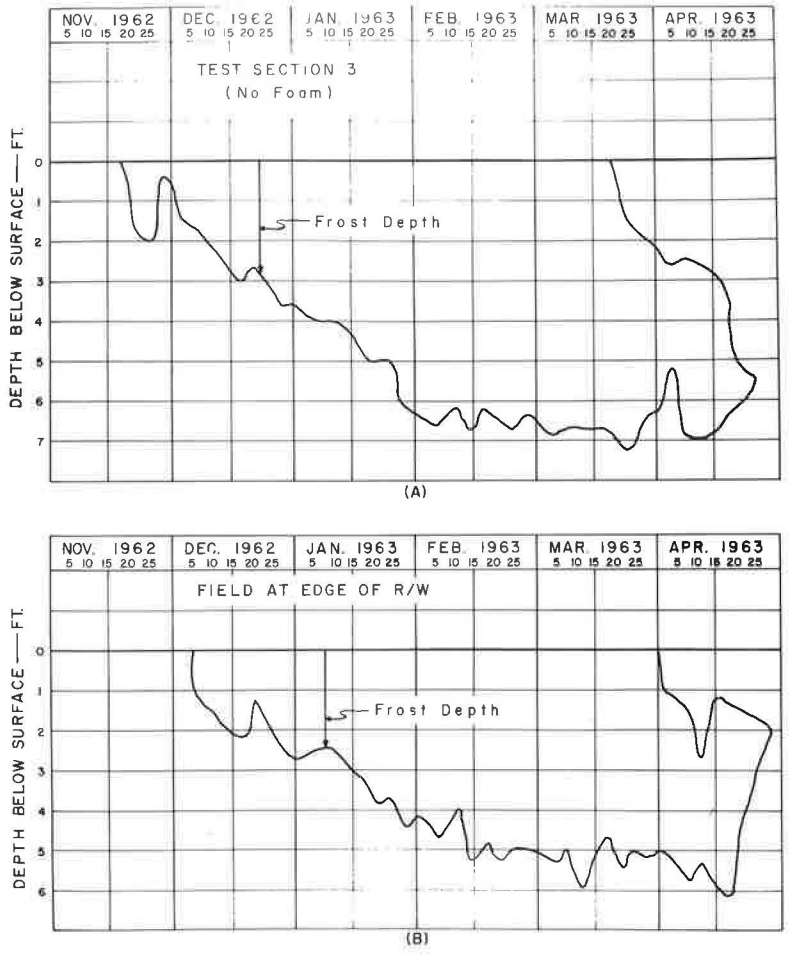

Figure 6. Variation in frost depth with time of year.

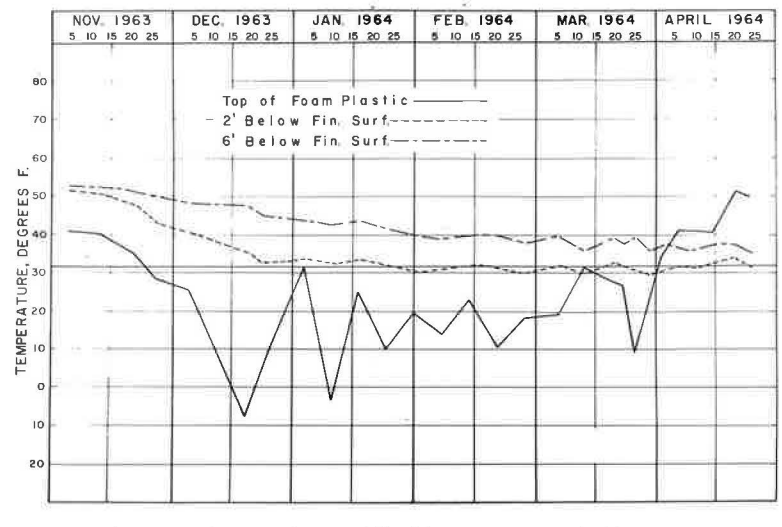

Figure 7. Comparison of temperature with time of year at three depths in section 1.

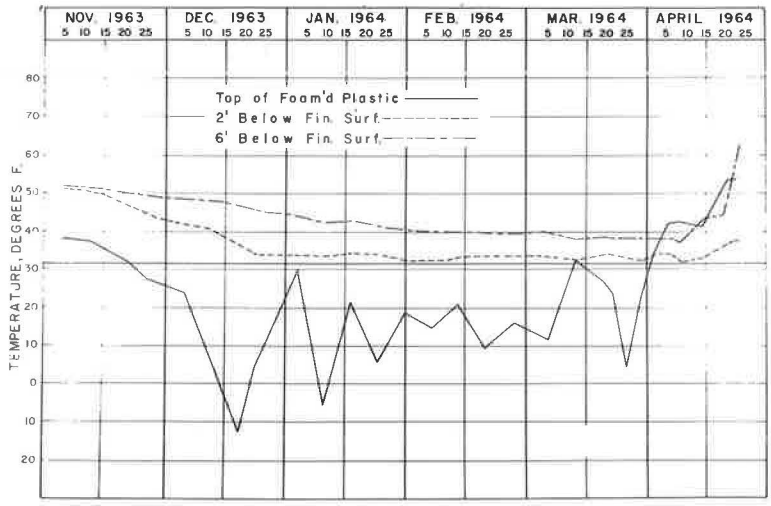

Figure 8. Comparison of temperature with time of year at three depths in section 2.

Figure 5a shows the temperature variations at a depth of 16 in. from pavement surface, immediately above the foamed plastic. The extremes in temperature are greater in the section containing foam than in the one which did not. Figure 5b shows temperature variations at a depth of 2 ft 0 in. which would be below the foamed plastic layer in sections 1 and 2. These measurements indicate that there is only slight frost penetration of the soil below the 2-in. foam and practically none below the $3\frac{1}{4}$-in. layer. The temperature below the $3\frac{1}{4}$-in. layer was never lower than 30 F and only reached 26 F under the 2-in. layer. In the control section, the temperature at this depth dropped to 2 F.

Figure 6 shows temperature variation in the control section and for a point in the prairie. The frost penetrated to a depth in excess of 7 ft in the road where there was no insulation and to a depth of about 6 ft in the prairie where there had been some snow cover.

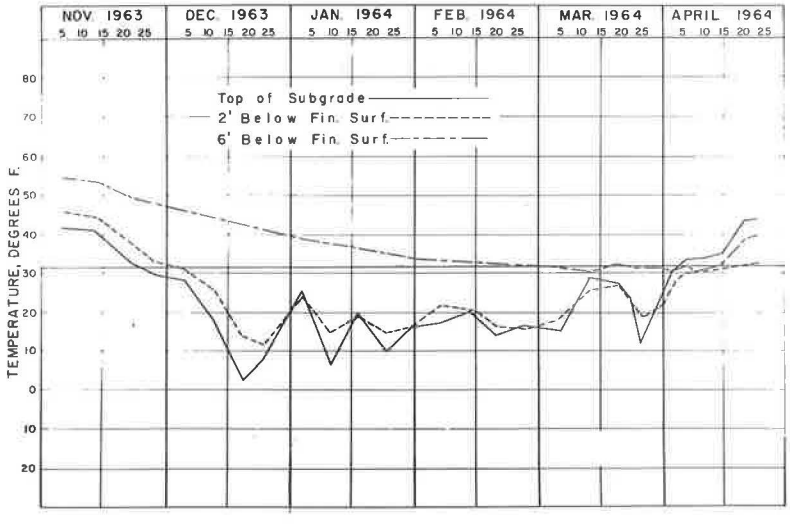

Figure 9. Comparison of temperature with time of year at three depths in section 3.

In Figure 7, the 1963-64 readings are plotted to show the comparison between temperatures at depths of 2 and 6 ft below the surface and the temperature above the foam for section 1. Figure 8 shows a comparison for section 2 and Figure 9 for section 3 which had no foamed plastic.

Excavation of several locations in the summer of 1964 indicated that the foamed plastic had not deteriorated or failed structurally following 2 yr of service. There was little moisture absorption and, except for the indentations of a few stones and discoloration of the upper surface, the plastic generally was unchanged since installation.

CONCLUSIONS

The continuously extruded polystyrene foam (Styrofoam) provided sufficient insulation at a 3¼-in. thickness to essentially prevent frost penetration into the subgrade. There was a slight depth of frost immediately below the 2-in. thick foamed plastic layer but it did not exceed a few inches.

Under 12 in. of gravel base course and a 4-in. bituminous surface, the foamed plastic was not affected by traffic loads. Construction traffic loads did not fail the plastic. Loaded gravel trucks were able to traverse the area without failure of the plastic when it was protected by 8 to 12 in. of gravel.

FUTURE RESEARCH

The experimental project described in this paper will continue to be observed and tested until it is removed to make way for the Winnipeg Floodway.

A new installation is nearly completed, on the west side of the Perimeter Highway around Winnipeg, which involves the insulation of a double steel arch culvert. A cross-sectional view of this installation is shown in Figure 10. The insulation used was a continuously extruded polystyrene foam with high density surface skins (Styrospan, Dow Chemical of Canada). It is hoped that this installation will yield useful information concerning differential frost heave at culverts due to the greater frost penetration usually encountered at culvert locations. The foam used in this project was 2 in. thick. The area was instrumented with thermocouples as in the previous test.

Further research is required to determine the structural value of foamed plastic in a highway. A project is presently under consideration incorporating this material into a highway section, protected by various depths of pavement structure.

ACKNOWLEDGMENTS

The author wishes to acknowledge the contribution of the Dow Chemical Company and Dow Chemical of Canada whose interest in this project and provision of essential information regarding the use of foamed plastic assisted greatly in the successful development and completion of this research installation.

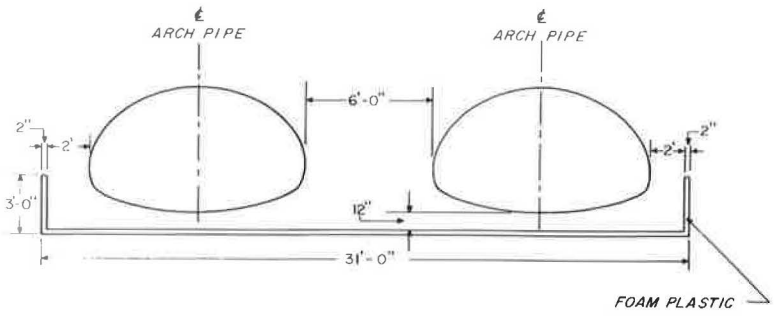

Figure 10. End elevation of arch pipe culvert and foam plastic insulation.

The contribution of R. N. Sharpe to this project is worthy of special recognition. His vision and his interest in the development of new highway design and construction techniques were responsible for this research project.

This project would not have been possible without the efforts of many members of the staff of the Materials and Research Section of the Manitoba Highways Branch. Acknowledgment of all individuals whose contributions are worthy of special mention is not practical.

Use of Insulating Layer to Attenuate Frost Action In Highway Pavements

M. D. OOSTERBAAN, and G. A. LEONARDS
Respectively, Dow Chemical Company, Midland, Michigan; and Purdue University

Conventional methods of treating the detrimental effects of frost action are aimed at replacing or altering the frost-susceptible soils and/or controlling the water supply. The use of a Styrofoam insulating layer to attenuate frost action to reduce the effect of the freezing temperatures has been under study for the past 5 yr. Styrofoam insulating layers have shown promising results under test in a new flexible pavement at Midland, Mich., in a new rigid pavement near West Union, Iowa, and in a maintenance treatment of severe frost heave in flexible pavement near Minneapolis, Minn. A relatively smooth subgrade surface is required on which to place the Styrofoam boards, and an 8-in. thick lift of granular material placed over the Styrofoam will support construction traffic.

•FROST ACTION occurs in the presence of frost-susceptible soils, freezing temperatures, and a supply of water. Therefore, all solutions to the problem of frost action must be aimed at reducing or removing entirely the effect of one or more of these factors (1).

The most common approach to minimizing the effects of frost action is to replace the frost-susceptible soils with nonfrost-susceptible soils and provide adequate drainage for the pavement structure. Other methods utilize a layer of high heat capacity (2), a layer that cuts off moisture movements (3), or chemicals that retard freezing of the soil water (1).

From the standpoint of initial cost, effectiveness, and permanence, none of these methods is generally applicable to solving the wide range of problems with frost action encountered in highway construction.

The use of an insulating layer for attenuating frost action in highway and airfield pavements has been under study by Purdue University and the Dow Chemical Co. for 5 yr. A small-scale field test using a different insulating material was reported by the U. S. Army Corps of Engineers in 1962 (7). The work done at Purdue makes use of polystyrene plastic foam (Styrofoam) as the insulating layer.

Full-scale field test installations have been made in the northern United States and in Canada: three in Michigan, and one each in Iowa, Minnesota, Maine, Ontario, and Manitoba. One installation in Michigan and one in Manitoba are presently in their third winter. The installations in Iowa and Minnesota and the second one in Michigan are now in the second winter of service. The Maine and Ontario installations and the last one in Michigan were constructed during the summer of 1964.

This paper covers the results of the original installation in Michigan (5) and briefly reviews the Iowa and Minnesota installations.

DEFINITIONS

The following terms are used in this paper (6):

Mean annual temperature. The average of the average annual temperatures for several years.

Paper sponsored by Committee on Frost Action.

Degree-days. The number of degree-days for any day is the difference between the average daily air temperature and 32 F.

Freezing index. The number of degree-days between the highest and lowest points on a curve of cumulative degree-days vs time for one freezing season. The index determined for air temperatures at 4.5 ft above the ground is commonly designated as the air freezing index, and that determined for temperatures immediately below a surface is known as the surface-freezing index. The surface-air freezing index is used here to define the freezing index determined for air temperatures $2\frac{1}{2}$ in. above the pavement surface.

Design freezing index. The average air freezing index of the three coldest winters in the latest 30 yr of record. If 30 yr of record are not available, the air freezing index for the coldest winter in the latest 10-yr period may be used.

Mean freezing index. The freezing index determined on the basis of mean temperatures. The period of record over which temperatures are averaged is usually a minimum of 10 yr, and preferably 30, and should be the latest available.

n-factor. The ratio of surface freezing index to air freezing index.

k-factor. Thermal conductivity in units of Btu-in./sq ft-hr-°F.

Styrofoam. A type of polystyrene extruded and expanded 40 times; manufactured by the Dow Chemical Co., Midland, Mich.

Tautochrone. Vertical temperature variation in a test section at one point in time.

FIELD INSTALLATION

The original full-scale field test of the applicability of a foamed plastic insulating layer to attenuate frost action was built as part of an access road to the Dow Chemical Company plant at Midland, Mich., in 1962. This installation is presented to show use of the insulating layer in the construction of new flexible pavement. All freight trucks entering and leaving the plant used this road. As shown in Figure 1, traffic could be shifted at will to pass over the test sections.

The soil in the area is part of the lacustrine lake bed clays that cover parts of Michigan. The Michigan State Highway Department places this soil in the Selkirk series. In the Unified Classification System the subgrade soil would be a CH material. It is a brown plastic clay with gray mottlings. The index properties of this soil are given in Table 1.

Design of Test Installation

The load limits in Michigan are 18 kips per single axle and 32 kips per tandem axle. For traffic volumes less than 2,000 veh/day, the Michigan State Highway Department (8) recommends that a pavement section totaling $28\frac{1}{2}$ in. be used where subgrade soils have a CBR of 5 and frost action is not considered a serious problem. The section

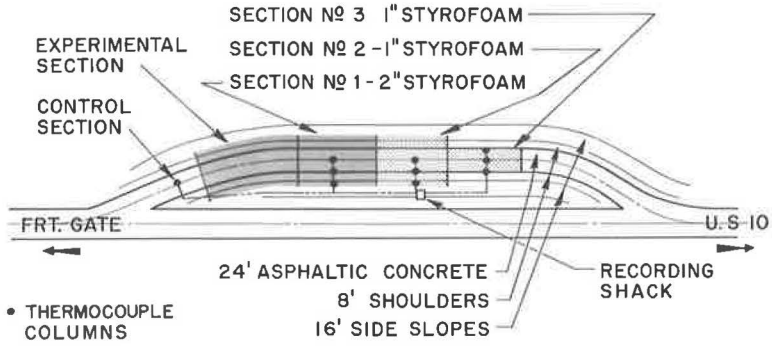

Figure 1. Plan of test installation, Midland, Mich.

TABLE 1

PROPERTIES OF SUBGRADE SOIL, MIDLAND, MICH.

Property	Value
Natural water content (%)	23-26
Liquid limit	55-60
Plastic limit	22-25
Plasticity index	30-38
% < No. 200 U.S. standard sieve	97
Clay fraction (% <0.002 mm, approx.)	70
In situ wet density (pcf)	122
Optimum density (standard proctor, pcf)	101
Optimum moisture content (%)	23
Soaked CBR	5-10

consists of a 2½-in. surface of asphaltic concrete, an 8-in. base of crushed gravel; and an 18-in. subbase of porous material Grade A. Where frost action is a problem, it is recommended that the subbase be increased 12 to 18 in. or more. A section with a 26-in. subbase was used as the control section. For the insulated test sections it was felt that frost action would not be a problem, hence the subbase thickness was reduced to 14 in.

McCammon (9) conducted a controlled model study which indicated that 1 in. of foamed plastic insulation could attenuate freezing temperatures at Midland if one-dimensional heat flow could be assured. Accordingly, two thicknesses of the insulating layer were used in the test sections—1 and 2 in.—and their widths were varied to define the limits within which one-dimensional heat flow might occur in the road. Section 1, with a 50-ft width and 2-in. thickness of the insulating layer, is shown in Figure 2; section 2, with a 50-ft width and 1-in. thickness, is shown in Figure 3; section 3, a 26-ft width and 1-in thickness, is shown in Figure 4.

Instrumentation to measure thermal performance during the winter months consisted of thermocouples. These were placed to give temperatures with depth at the centerline, at the edge of pavement, and at the edge of the insulating layer of the three test sections. The thermocouples were connected to Minneapolis-Honeywell strip-chart recorders. Temperatures were recorded at intervals of 2 to 5 days, usually between 8 and 10 a.m.

Temperature Observations and Results

Temperature observations were made at the test installation during the 1962-1963 and 1963-1964 winters. The results of the 1962-1963 winter are presented here since they give performance during a winter that was more severe than the usual design condition for the Midland, Mich., area. The results of the mild 1963-1964 winter were

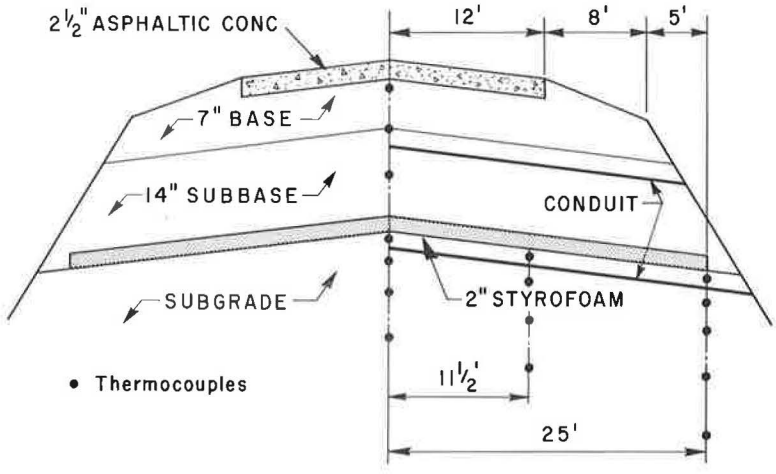

Figure 2. Instrumentation and cross-section of section 1, Midland, Mich.

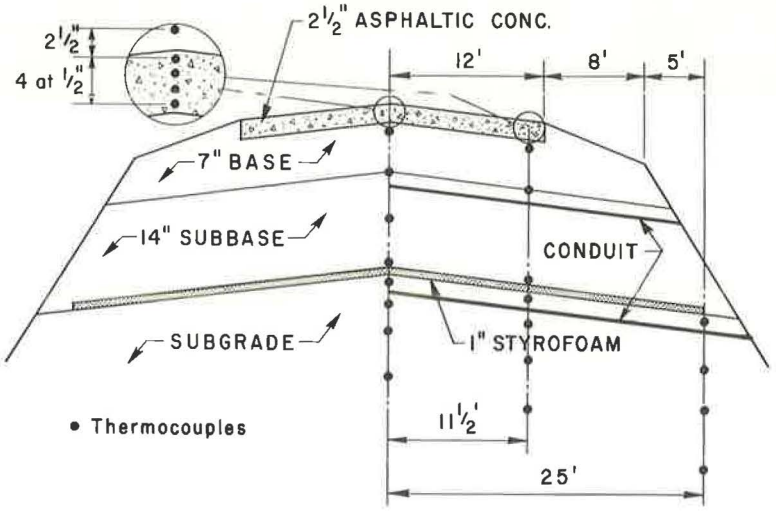

Figure 3. Instrumentation and cross-section of section 2, Midland, Mich.

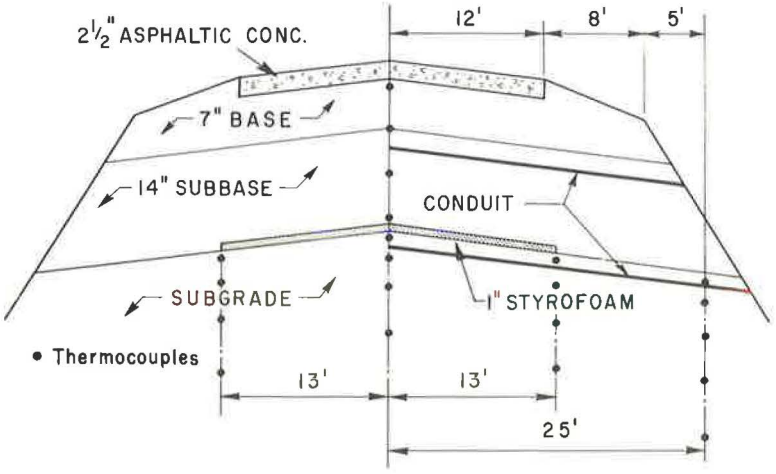

Figure 4. Instrumentation and cross-section of section 3, Midland, Mich.

similar but did not show frost penetrations as deep or temperatures as severe as recorded the previous winter. However, they are summarized later for comparison purposes.

The mean freezing index for the Midland area is 850 degree-days. The design freezing index for the area is 1,300 degree-days and usually spans 110 days. The mean annual temperature is 44 F at this location (10).

The 1962-1963 winter was the coldest in 26 yr at the Midland weather station. A freezing index of 1,263 degree-days was recorded over a 99-day period as shown in Figure 5. At the Tri-City Airport, some 10 mi southeast of Midland, a freezing index of 1,622 degree-days was recorded over 107 days. The Midland weather station is located some 15 ft from the Tittabawasee River which undoubtedly moderates the temperature and accounts for the 360-degree-day difference in the freezing index.

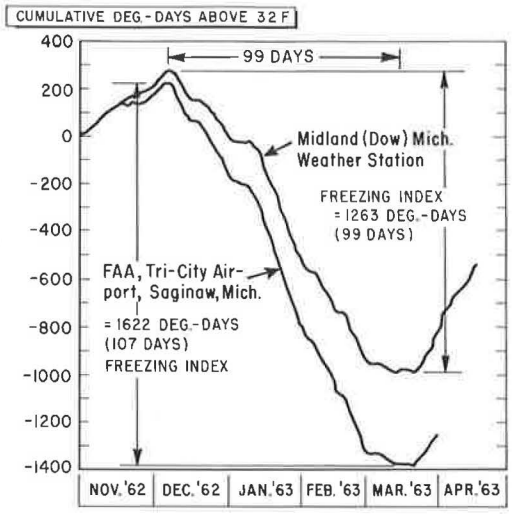

Figure 5. Cumulative degree-days above and below 32 F at Midland and Tri-City Airport weather stations.

The test installation is ½ mi from the Midland weather station and about 100 yd from the river. The surface-air freezing index determined from temperatures recorded at the test installation was 1,302 degree-days. The surface freezing index was found to be 1,261 degree-days.

n-Factors

Kersten's study of n-factors in Minnesota showed a range from 0.6 to 0.8 (12). Sanger, in discussion of Kersten's paper, states that an n-factor of 0.9 ± 0.05 was found from a statistical analysis of U. S. Army Corps of Engineers' data. Quinn and Lobacz found n-factors of 0.98 for an insulated portland cement concrete slab and 0.66 and 0.71 for uninsulated portland cement concrete slabs (7).

Using the air freezing index of the Midland weather station, an n-factor of approximately 1.00 is obtained; using the air freezing index of the Tri-City Airport, an n-factor of 0.78 is obtained; and using the surface-air freezing index at the test site, an n-factor of 0.97 is obtained. These values indicate that local environmental conditions at a weather station can materially affect the computed n-factor.

Temperatures in Test Sections

1962-1963 Winter.—In the interest of brevity, only those measurements defining progressive temperature changes at critical points in each test section will be presented. The times for which tautochrones are shown correspond to:

1. End of construction;
2. After start of freezing season;
3, 4, 5. Times when lowest temperatures were recorded above and below the insulating layer;
6. End of freezing season; and
7. Approximate time of spring breakup.

In section 1 (2-in. Styrofoam), the temperature above the insulating layer reached a minimum of 8 F on Jan. 15, as shown in Figure 6. At the same time, the temperature below the insulation was 42.5 F, or a differential of 17 F/in. of insulation. The minimum temperature below the insulation, 38 F, was recorded March 1.

It is of interest to note that at the start of the freezing season, Dec. 6, the temperature at the top of the subgrade was 50 F. This is 6 F above the mean annual temperature for this area.

At the centerline of section 2 (1-in. Styrofoam), the temperatures shown in Figure 7 were recorded. On Jan. 28, the minimum temperature above the insulation was 14 F and below the insulating layer was 31.7 F. Again, the differential was 17 F/in. of insulation.

If 32 F is considered the freezing point, although undercooling and freezing point depressions are known to exist, the temperature gradients indicate a "frost penetration" of about 2 in. (noted by the arrow on Figure 7.) The existence of frost was verified nearly a month later, on Feb. 20, when a core of the subgrade revealed randomly oriented ice lenses about 2 mm thick to a depth of ½ in. below the insulation. The temperature recorded just below the insulation at this time was 32.8 F. This discrepancy is not incompatible with the accuracy of the measurements, which is believed to be on the order of 1 F.

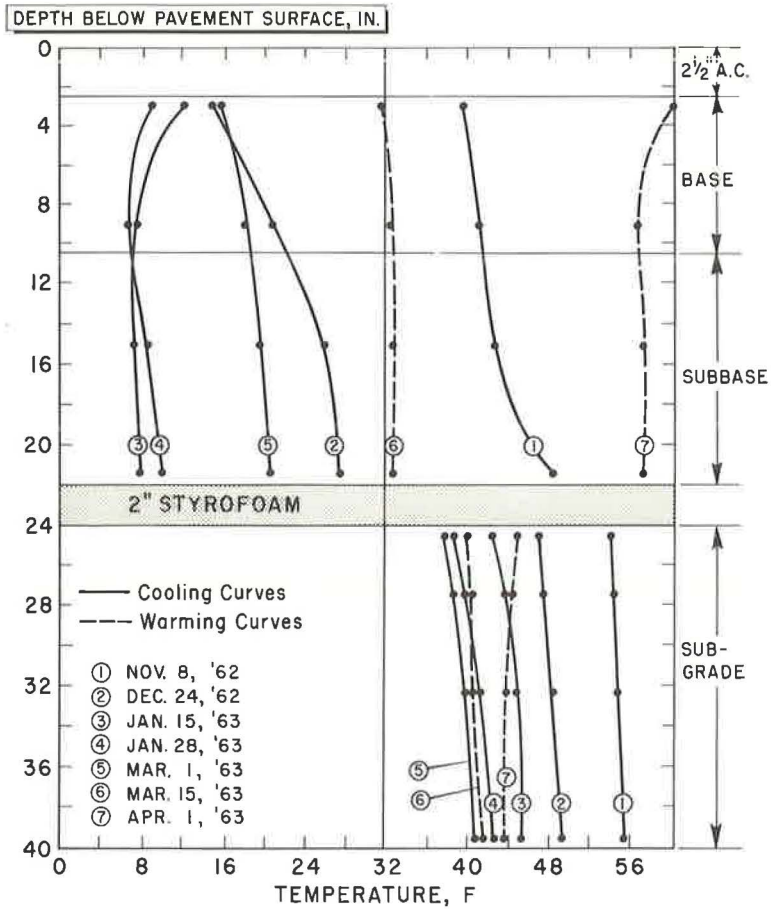

Figure 6. Temperatures at selected times, section 1 centerline (2-in. Styrofoam insulation), Midland, Mich.

The temperatures recorded at the centerline of section 3 were similar to those recorded at the centerline of section 2.

The depth of the 32 F isotherm was interpreted from the recorded data and is plotted in Figures 8, 9, and 10.

The shaded areas in Figure 8 show the zones within which the temperature dropped below 32 F at the centerline, edge of pavement, and edge of insulation in section 1. No frost penetration was found beneath the 2-in. insulating layer at the centerline or pavement edge where one-dimensional heat flow was occurring. At the edge of the insulation (5 ft out from the shoulder), two-dimensional heat flow occurred and the 32 F isotherm penetrated to 20 in. below the edge of the insulation by March 15.

Data similar to that of Figure 8, but for section 2, are shown in Figure 9. "Frost" penetrated to a maximum of 6 in. below the insulating layer at the edge of pavement about March 1. About Feb. 1, temperatures below 32 F were also noted at this same point to a depth of 3 in. These "frost" penetrations lasted for 5 to 10 days (until the surface conditions became warmer and the heat flow from the earth was sufficient to raise the temperature above freezing). At the edge of the insulating layer, frost penetrated to a depth of 20 in. in a situation similar to that found in section 1.

In section 3, where the 1-in. insulating layer extended only 1 ft beyond the pavement edge, the frost penetration at the centerline was found to be similar to that of section 2

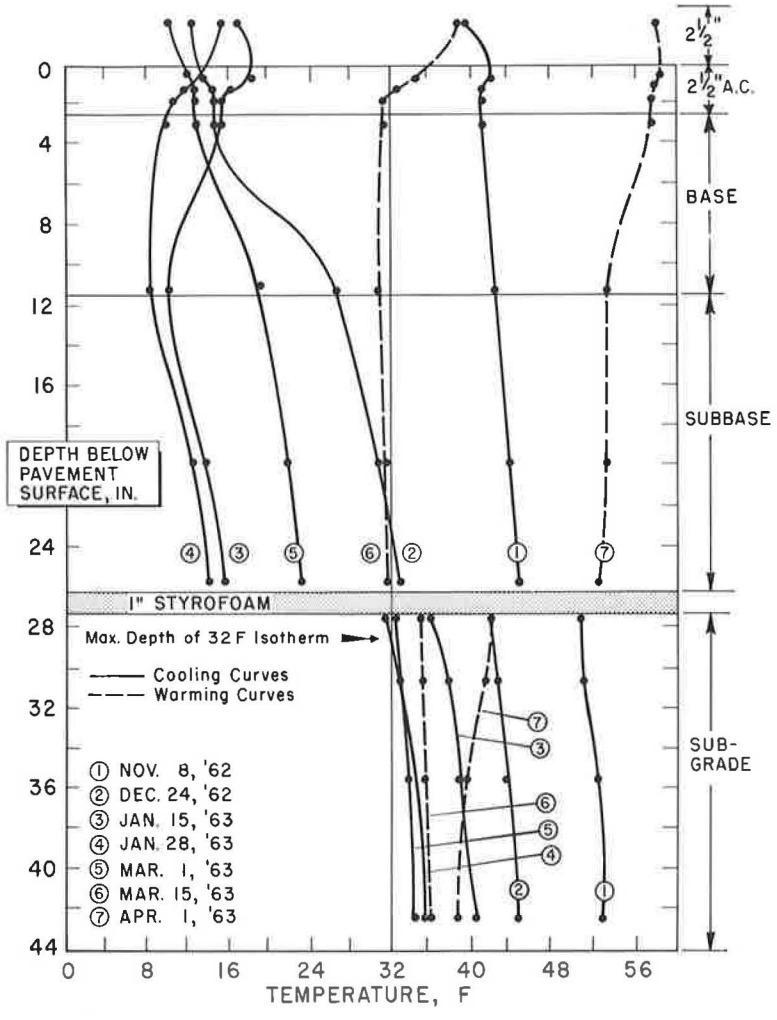

Figure 7. Temperatures at selected times, section 2 centerline (1-in. Styrofoam insulation), Midland, Mich.

(Fig. 10). At the edge of the insulating layer (or the edge of pavement) "frost" penetrated 15 in. on the left and 19 in. on the right into the subgrade—a situation again very similar to that found at the edge of the insulation in sections 1 and 2.

Frost penetration at the edge of the pavement was 15 to 19 in. below the insulating layer throughout February. This was verified by a soil core taken Feb. 20 at the right edge of the pavement. The core showed ice lenses in the subgrade to a depth of 18 in. These were $\frac{1}{16}$ to $\frac{1}{8}$ in. thick and occurred at intervals of about $\frac{1}{2}$ in., totaling approximately $\frac{1}{2}$ in. of ice. The moisture contents in this zone had increased some 20 percent from the moisture contents at the time of construction.

Heaves of about 0.40 in. were found at the pavement edge in section 3, but no movement was found at the centerline where frost penetration was negligible. This is compatible with the ice formation found in the soil cores.

Some selected temperatures recorded in the control section are shown in Figure 11. The minimum temperature recorded at the top of the subgrade was 27 F on Feb. 27.

To estimate the full depth of frost penetration in the control section, an extrapolation was made based on a temperature gradient of 3 F/ft. This placed the frost penetration at $4\frac{1}{2}$ to 5 ft. From tautochrones 7 and 8 (Fig. 11) it is estimated that frost did not leave this section until April 2.

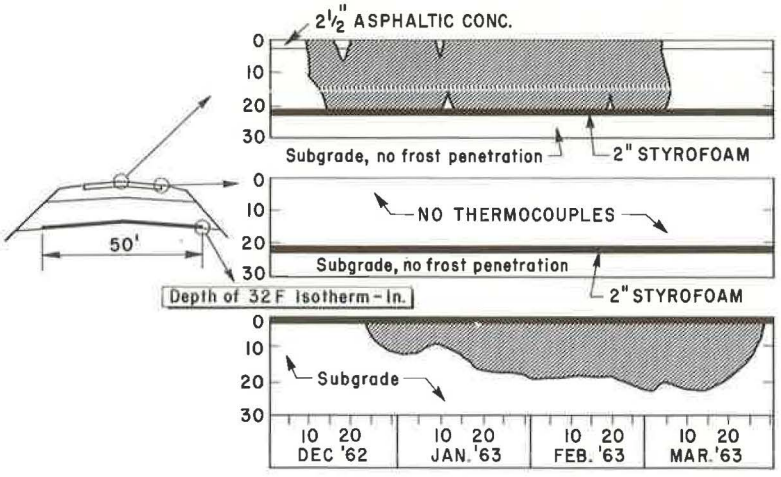

Figure 8. Depth of 32 F isotherm with time, section 1, Midland, Mich.

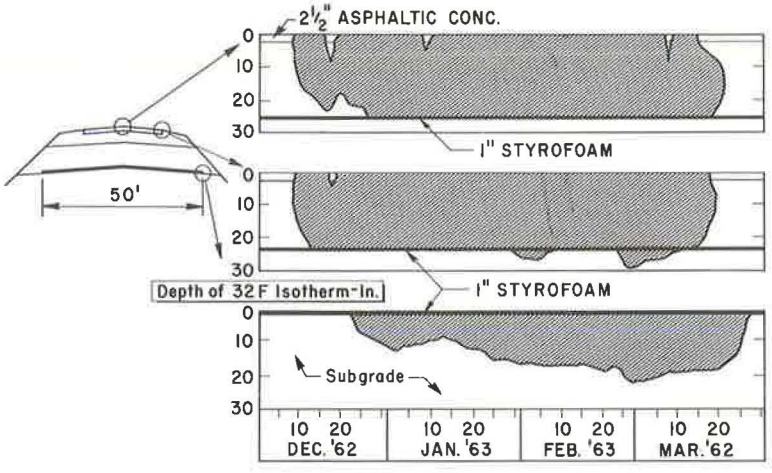

Figure 9. Depth of 32 F isotherm with time, section 2, Midland, Mich.

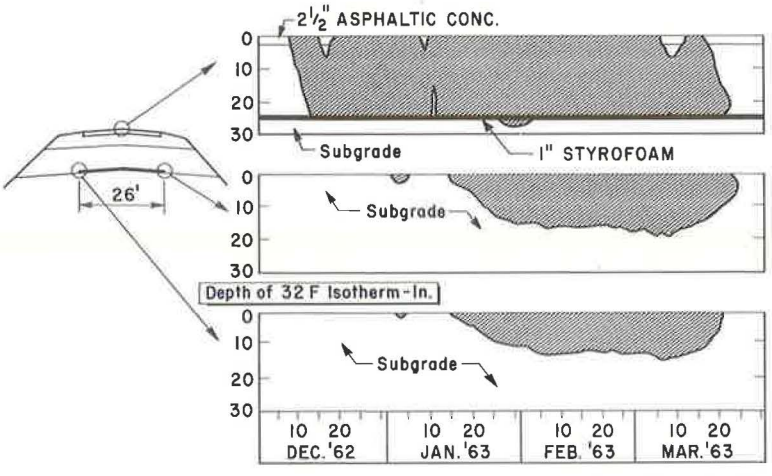

Figure 10. Depth of 32 F isotherm with time, section 3, Midland, Mich.

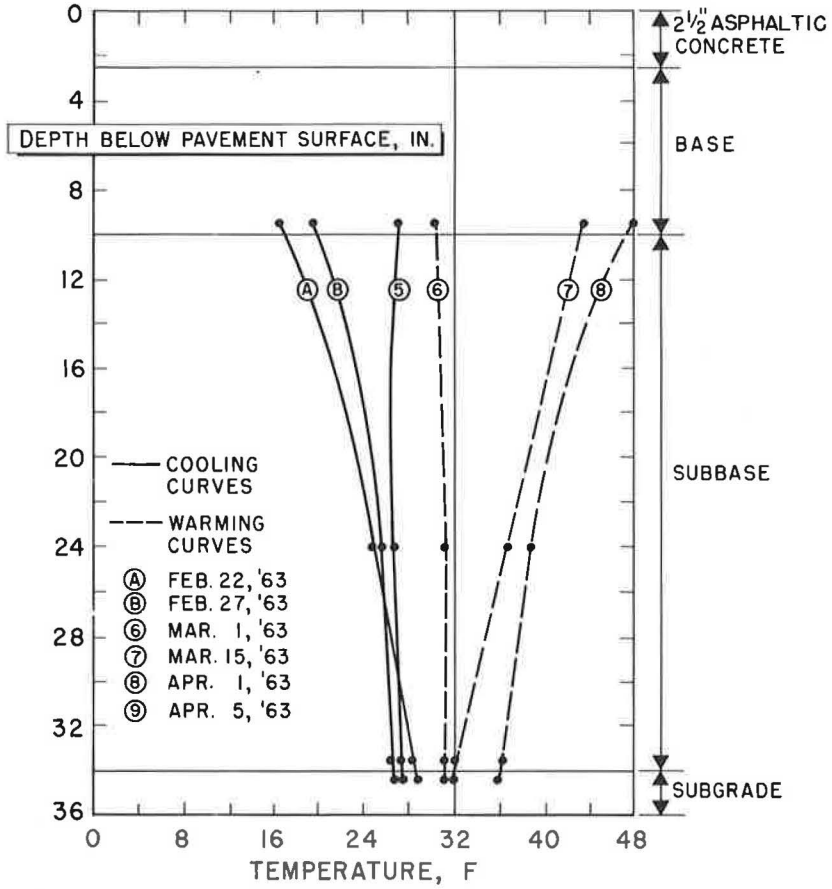

Figure 11. Temperatures at selected times, control section centerline, Midland, Mich.

1963-1964 Winter.—This winter was considerably milder than the previous one. A freezing index of 700 degree-days was recorded at the Midland weather station and 689 degree-days at the Tri-City Airport weather station over a 91-day freezing season. This is some 100 degree-days less than the mean freezing index for the area and 560 to 980 less than those recorded the previous winter.

The temperatures recorded below the insulating layer in the insulated test sections were 2 to 5 F above those recorded the previous winter. The frost penetration into the subgrade at the edge of the insulating layer (edge of pavement) in section 3 was 5 to 10 in. In the control section the depth of frost penetration into the subgrade was estimated to be 6 to 10 in., or one-third of that found the previous winter.

Moisture Conditions in Insulated Sections

The effect of the insulating layer on the moisture regime in the pavement structure was an intriguing question at the start of this investigation. Colman soil moisture cells (Model 351, Beckman Instruments, Inc.) were installed in sections 2 and 3 in an attempt to give a picture of the changes that might take place. It soon became apparent that prior calibration curves were invalid. Hence, soil cores were taken at various times to give the desired data.

Figure 12 shows the moisture contents obtained from soil cores in section 2. Above the insulating layer, the moisture content of the subbase increased substantially during the winter months. The water contents (frozen) of 14 to 17 percent recorded Feb. 20, 1963, are nearly equivalent to 100 percent saturation for this soil. When the ice in the

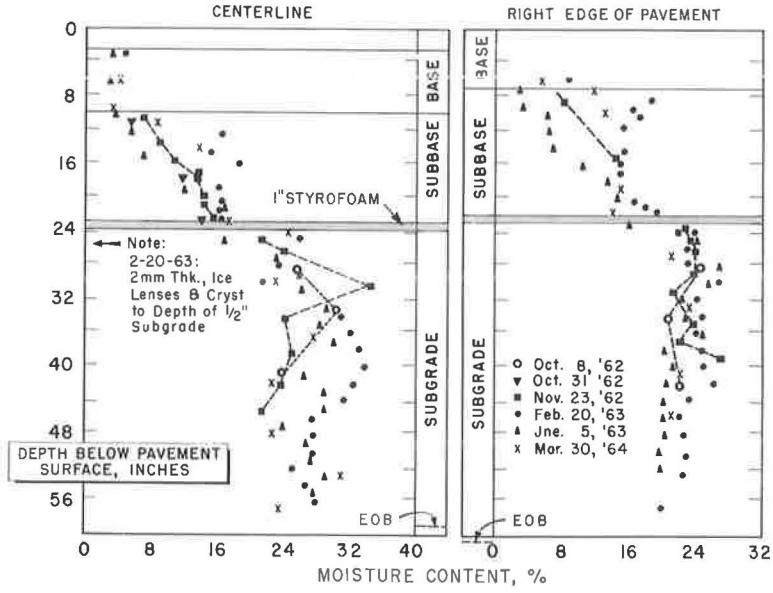

Figure 12. Change of moisture content with time, section 2, Midland, Mich.

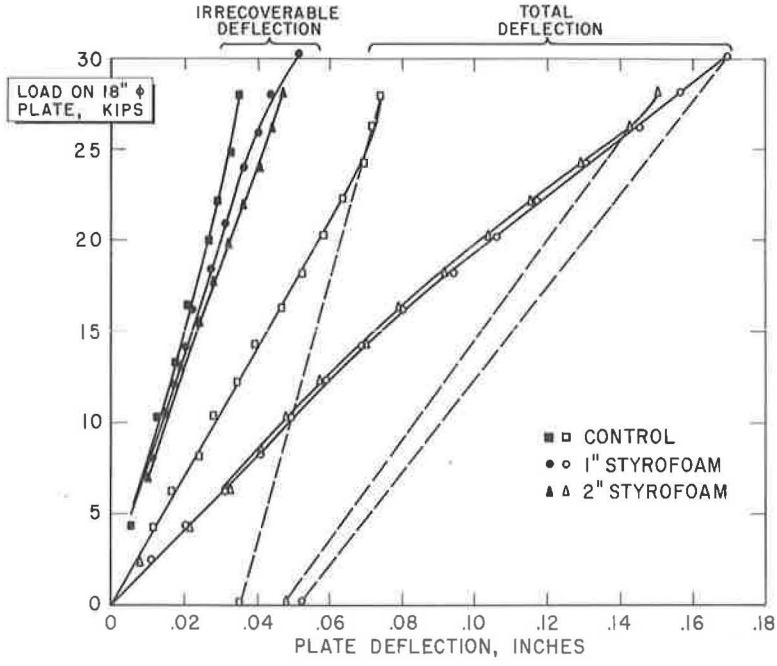

Figure 13. Results of plate loading tests on test sections, spring 1964 (after 2 winters of service), Midland, Mich.

subbase melted at the end of the freezing season, it undoubtedly contributed to some loss of supporting strength in the pavement structure. As ice melted from the shoulders, the subbase drained and the capacity of the pavement was restored substantially to its initial condition, as indicated by load test data.

TABLE 2

k-FACTORS AND WATER PICKUP OF STYROFOAM INSULATING LAYER, MIDLAND TEST INSTALLATION[a]

Layer Thickness (in.)	Water Pickup (% by vol)	k-Factor $\left(\frac{\text{Btu-in.}}{\text{sq ft-hr-}^\circ\text{F}}\right)$		
		Wet	Dry	Δk
1	0.65	0.27	0.25	0.02
2.1	0.34	0.25	0.24	0.01

[a]After two winters ($1\frac{1}{2}$ yr) of service.

Just below the insulating layer, moisture contents at the centerline increased about 8 percent during the freezing season, but by June 5 they had essentially returned to the initial condition.

Load-Carrying Capacity

To assess the comparative load-carrying capacity of the insulated and uninsulated test sections, load tests were performed immediately after construction (November 1962), in the spring of 1963, and again in the spring of 1964. A typical set of results is shown in Figure 13.

From the load vs total deflection curves, it is evident that the insulating layer increases the temporary deflection of the pavement materially; however, for wheel loads under 10 kips the deflection is less than 0.05 in., which is considered tolerable in the case of flexible pavements (13).

The irrecoverable deformation vs load curves show that the support provided by the insulated and uninsulated sections are comparable, even though the control section has an added subbase thickness of 12 in. This suggests that the Styrofoam provides a cushioning effect which distributes subgrade stresses more evenly, thereby adding a useful structural function to its insulating qualities. Further studies of the structural advantages which may accrue through the use of a Styrofoam insulating layer are currently in progress.

Insulating Layer Properties

Samples of the insulating layer were removed on April 4, 1964, to determine the physical properties of the insulating layer after two winters of service. The effectiveness of an insulating layer is dependent on the permanence of its thermal properties. The k-factors for wet and dry specimens are given in Table 2.

The wet k-factors were determined for the samples as they were taken from the test installation. After drying to remove the water in the specimen, the k-factor test was rerun to determine the effect of moisture pickup.

The type of insulating layer used in this test—Styrofoam SM brand insulation—is especially resistant to moisture pickup and, hence, should not change appreciably in thermal conductivity. The water pickup (percent by volume) by these specimens was small and the changes in k-factor that resulted from this minor amount of moisture pickup were not detected by the k-factor test. The limit of accuracy of the test is 0.01 Btu-in./sq ft-hr-°F.

Further testing along this line is being conducted by the Dow Chemical Co. using accelerated freeze-thaw tests to determine the freeze-thaw durability of various insulating materials that might be used to attenuate frost action beneath pavements.

Summary and Conclusions

The first full-scale field test installation using a foamed plastic insulating layer in a flexible pavement showed that:

1. A 1-in. thickness of Styrofoam insulation effectively prevented frost action in the subgrade of a flexible pavement in an area where the freezing index reached 1,600 degree-days.
2. A width of insulation some distance beyond the pavement edge is required to prevent frost formation beneath the pavement. Studies are presently under way to determine the lateral extent of the frozen zone at the edge of the insulating layer.
3. Frost penetrations beneath a foamed plastic insulating layer to a depth of 6 in. for a short period of time did not appear to be detrimental. Heat flow from the earth dissipated the ice formed as soon as a temporary cold cycle passes.
4. The excess moisture that collects in the subbase during the freezing season is responsible for some of the loss in bearing capacity during spring breakup.
5. The presence of an insulating layer that is essentially impermeable to moisture did not cause moisture concentrations in the subgrade over a period of 2 yr.
6. The insulating layer showed negligible moisture pickup and, hence, no significant change in thermal conductivity after two winters of effective performance.
7. The foamed plastic insulating layer reduced the thickness of the flexible pavement structure normally required for satisfactory performance in frost areas. Studies are currently under way to establish its economic applicability.

IOWA TEST INSTALLATION

The Iowa test installation was constructed in 1963 2 mi west of West Union, Iowa, on US 18. The original concrete pavement was badly cracked, and in certain areas had experienced perennial frost heaves. In these areas the conventional subgrade treatment was to remove the subgrade soil for a depth of 3 ft and replace it with a nonfrost-susceptible material. In one of these treatment areas a Styrofoam insulating layer 1½ in. thick was used in lieu of the 3 ft of nonfrost-susceptible material for 250 ft of the 450-ft treatment.

Figure 14 shows the cross-sections and the instrumentation placed in the two treatments. The conventional treatment served as the control section in this installation. Another section similar to the insulated section, but having two layers of the insulating material, each ¾ in. thick, was also instrumented.

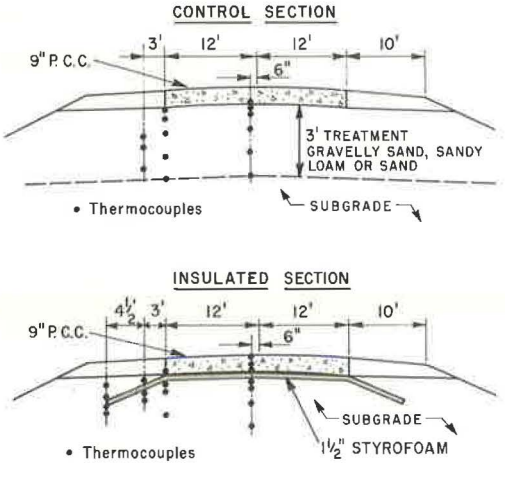

Figure 14. Cross-sections and thermocouples of control and insulated P.C.C. Sections, West Union, Iowa.

The freezing index for the 1963-1964 winter at Waterloo, Iowa, some 40 mi southeast of the test installation, was 1,217 degree-days over 130 days. An air thermocouple at the site furnished data for computing a 1,461 degree-day freezing index, also over a period of 130 days. The mean freezing index for this area is 1,100 degree-days over a 105-day period and the design freezing index was 1,700 degree-days (10).

Temperatures at this installation were recorded from 24 thermocouples at 2-hr intervals by a strip-chart recorder. At weekly intervals, data were taken for 1 day from 24 additional thermocouples.

The temperatures recorded above and below the 1½-in. Styrofoam insulating layer during the 1963-1964 winter are shown in Figure 15. The 8:00 a.m. tem-

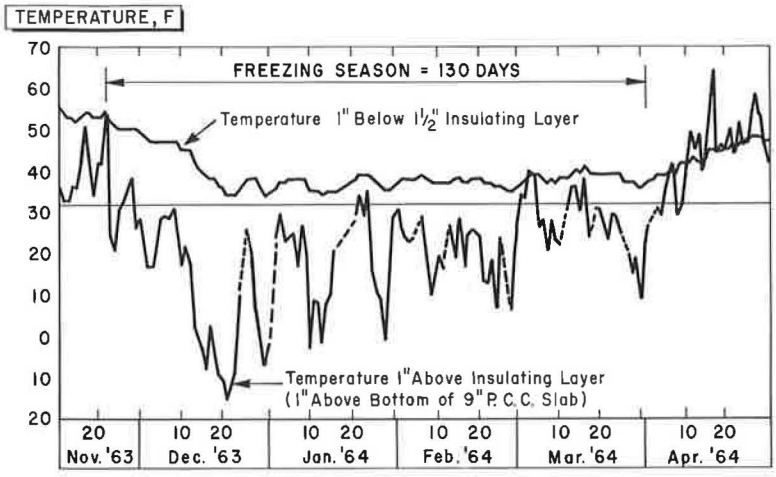

Figure 15. Temperatures above and below insulating layer throughout 1963-1964 freezing season at 8:00 a.m., West Union, Iowa.

peratures were chosen as being representative of the performance of the insulating layer. During the freezing season the temperature above the 1½-in. insulating layer dropped as low as -15 F. The temperature below the insulating layer never dropped below 34 F.

Intermittently, heat flow from the earth and relatively warmer surface temperatures caused the temperature below the insulating layer to rise 3 to 5 F.

Freezing indices were computed from the data of several thermocouples in the insulated and control sections using a computer program developed by Straub and Wegmann (11). The freezing indices computed from these thermocouples are shown in Figure 16.

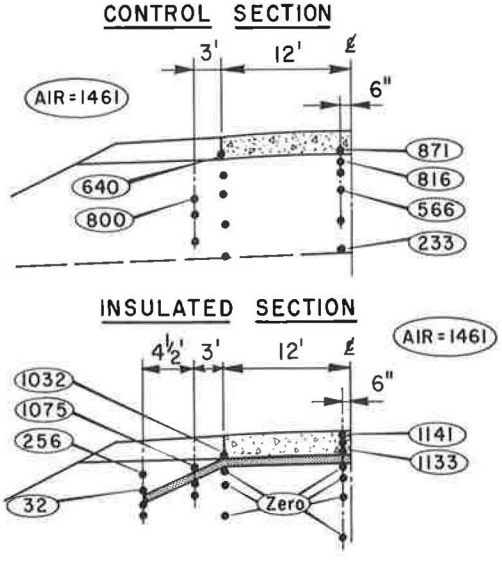

Figure 16. Computed freezing indices at various points in control and insulated sections, West Union, Iowa.

In the control section, the freezing index at the bottom of the treatment (-46 in.) was 233 degree-days. Extrapolation of the tautochrone below this point at Jan. 15 places the frost line at -5 ft.

The n-factor for the insulated section was 0.77. Based on an increase of 16 degree-days per inch of concrete (7), the surface freezing index of the control section would have been 983 degree-days. This would give an n-factor of 0.67. A smaller gradient, as the 10 degree-days presently recommended by the Corps of Engineers (7), would give an n-factor of 0.65. These values are similar to those reported by Kersten from his Minnesota study (12). In the absence of an air thermocouple near the pavement surface, a surface air freezing index (and its corresponding n-factor) could not be computed.

During the first year of service, the insulated section (with the concrete directly on the insulating layer) showed no visual evidence of structural deterioration. In the early summer of 1964, 3 in. of asphaltic concrete were placed on US 18 throughout the area under study so that the pavement section now totals 12 in.

Moisture samples taken from the control and insulated sections in April 1964 showed that the moisture content of the silty clay subgrade ranged from 15 to 17 percent. Original specifications required compaction at 18 percent moisture.

Centerline elevations taken during February 1964 showed that since December the section of conventional treatment had heaved 0.03 ft, the Styrofoam treatment heaved 0.02 ft, and an adjacent untreated area had heaved 0.08 ft. In May the elevations were about equal to those recorded in December. It is considered that the apparent anomaly of frost heave occurring in the Styrofoam area, where no freezing temperatures were recorded in the subgrade, is the result of leveling error.

Summary and Conclusions

1. A 1½-in. Styrofoam insulating layer placed directly on a frost susceptible subgrade prevented frost penetration beneath a rigid pavement during a normal winter in northeastern Iowa.
2. Based on the temperatures recorded in the subgrade of both frost action treatments and on observations of comparative performance, the 1½-in. insulating layer effectively replaced more than 3 ft of granular material.

MINNESOTA INSTALLATION

The installation in Minnesota was made during 1963 as a maintenance operation by the Minnesota Highway Department on Trunk Highway 25 about 25 mi southwest of Minneapolis. This highway had experienced frost heaves of 0.2 to 0.4 ft, developed chuckholes, and required perennial spring repairs. The original pavement section was, in general, 6 in. of bituminous concrete, 10 in. of loamy sand, and a sandy, silty, clay loam subgrade.

In the two heave areas treated (48 and 68 ft long), the pavement was removed to a depth of 23½-in. Then a 2-in. thickness of Styrofoam, 30 ft wide, was placed on the subgrade. This was then covered by 17 in. of sand and gravel and 3 in. of bituminous concrete. An additional 1½ in. of bituminous concrete was then placed as resurfacing for the entire area.

Thermocouples were installed to give an indication of performance. These were read infrequently and gave only enough data to determine that freezing did not occur below the insulating layer during the 1963-1964 winter, which had a freezing index of 1,500 degree-days over 124 days.

During the winter, levels run through the treated areas showed no change in elevation. However, at the end of the insulating layer treatment, heaves up to 0.35 ft were recorded.

In general, this installation performed well and has given assurance that the insulating layer can be especially helpful in severe problem areas.

SUMMARY OF CURRENT CONSTRUCTION TECHNIQUES

Subgrade

The use of Styrofoam brand insulation boards requires that the subgrade be fine-graded so that deviations from a 10-ft straightedge are in the range of ± ½ in. This is intended to prevent puncture damage from clods of soil and cracking damage if an uneven support condition exists when granular materials are placed on the Styrofoam. Figure 17 shows Styrofoam being placed over an acceptable subgrade at a Michigan installation.

For a rigid pavement, the usual grading requirements for placing concrete are sufficient and the Styrofoam insulation can be placed without additional work. Figure 18 shows Styrofoam being placed at the Iowa installation.

Alignment

The long dimension of the 2- by 8-ft Styrofoam boards is kept parallel to the centerline by means of a stringline. The boards are secured in place by driving three or four

Figure 17. Styrofoam insulating layer being placed on graded subgrade for flexible pavement in Michigan.

Figure 18. Placement of Styrofoam insulating layer for concrete pavement in Iowa.

pointed wooden dowels (¼ by 6 in.) through the foam into the subgrade as shown in Figure 17. This not only keeps the boards in place during placement operations, but also enables the use of uncaulked butt joints between boards.

In the original installation at Midland, the thermal efficiency of various joints was investigated. It was found that butt joints, with a gap less than ¼ in. between boards, allowed the temperature at the bottom of the joint to fall only several degrees below the temperature recorded below a perfectly sealed, insulating joint. It is felt that the cost involved in sealing and insulating a joint does not justify the small increase of thermal efficiency that would be realized.

Good alignment and tight joints are maintained by working outward from the string line in a step pattern and driving the wooden skewers at an angle to keep the board being placed from drifting away from those placed previously. Staggering the joints also helps to maintain alignment and tight joints. Figure 17 also shows these details.

Labor used on these installations have been primarily contracter's personnel. However, in one case the laborers were obtained from the local unemployment office. Even with these inexperienced people, there was no problem in obtaining the desired quality of workmanship. The installation techniques were explained and demonstrated in a few minutes.

Figure 19. Placement of concrete on Styrofoam insulating layer in Iowa.

Figure 20. Spreading subbase to 8-in. depth on Styrofoam insulating layer in Michigan.

Pavement Structure Above Styrofoam

For a rigid pavement the insulation is placed inside conventional concrete paving forms and the concrete is placed directly on the Styrofoam as shown in Figure 19. After

the forms have been removed the shoulder area is graded and the Styrofoam boards to insulate the shoulder area are butted against those at the bottom of the slab.

For a flexible pavement the granular material in the layer immediately above the Styrofoam is either end dumped at the edge of the treated section or spread alongside the insulation. A bulldozer or grader is then used to spread the granular material over the Styrofoam in a layer at least 8 in. thick as shown in Figure 20. This thickness is required to prevent excessive stress on the Styrofoam by construction equipment. This lift can then be compacted or used as a roadway for the trucks or earthmoving equipment hauling granular material. Vibratory compaction by a plate-type compactor is recommended because of its efficiency and relatively light weight, although other methods have been used to obtain the required density.

At this point normal construction equipment and techniques required for placement of the remainder of the pavement structure can be used without danger of damaging the Styrofoam insulating layer.

REFERENCES

1. Frost Action in Soils, A Symposium. Highway Research Board Spec. Rept. 2, 1952. 385 pp.
2. Skaven-Haug, Sv. The Norwegian State Railways' Measures Against Frost Heaving. Highway Research Board Spec. Rept. 2, pp. 348-356, 1952.
3. Bell, J. R., and Yoder, E. J. Plastic Moisture Barriers for Highway Subgrade Protection. Highway Research Board Proc., Vol. 36, pp. 713-735, 1957.
4. Aldrich, H. P., Jr. Frost Penetration Below Highway and Airfield Pavements. Highway Research Board Bull. 135, pp. 124-149, 1956.
5. Oosterbaan, M. D. Investigation of Foamed Plastic as an Insulating Layer in Highway Pavements. M.S.C.E. thesis, Purdue Univ., 1963.
6. Frost and Permafrost Definitions. Highway Research Board Bull. 111, pp. 107-110, 1955.
7. Quinn, W. F., and Lobacz, E. F. Frost Penetration Beneath Concrete Slabs Maintained Free of Snow and Ice, With and Without Insulation. Highway Research Board Bull. 331, pp. 98-115, 1962.
8. Michigan State Highway Department. Field Manual of Soil Engineering. 4th Ed., 1960.
9. McCammon, N. R. Experimental Investigation of the Rate of Frost Penetration in Clay. M.S.C.E. thesis, Purdue Univ., 1961.
10. Pavement Design for Frost Conditions. U.S. Army Corps of Engineers, Rept. EM 1110-1-306, 1962.
11. Straub, A. L., and Wegmann, F. J. The Determination of Freezing Index Values. Highway Research Record No. 68, pp. 17-30, 1965.
12. Kersten, M. S. Frost Penetration: Relationship to Air Temperatures and Other Factors. Highway Research Board Bull. 225, pp. 45-80, 1959.
13. McLeod, N. W. Some Notes on Pavement Structural Design. Highway Research Record No. 13, pp. 66-141, 1963.

Frost-Heaving Pressures

P. HOEKSTRA, E. CHAMBERLAIN, and T. FRATE
Respectively, Research Soil Physicist and Civil Engineers,
U. S. Army Cold Regions Research and Engineering Laboratory,
Hanover, New Hampshire

Considerable pressure develops on freezing a saturated soil in an open system from the top down. The pressure is the result of the surface energy of a curved ice-water interface. The curvature of the interface is necessary for ice to proliferate through the soil pores and is related to the pore size distribution of the soil.

The test chamber used is designed to minimize the friction of the soil with the wall. An accurate control of heat removal is obtained by thermoelectric cooling. A load cell placed on top of the sample is used to measure the pressure developed and at the same time prevents heaving of the sample. Measurement of the pressure on a layered sample shows that the pressure develops at the freezing front. Results on several soils indicate that each soil develops a characteristic maximum pressure. For each soil used, the water content vs tension curve is given and the maximum pressure is related to this curve.

•A SOIL frozen from the top down can lift a considerable load. This phenomenon is not related to the crystallization pressure that water develops on being frozen in a closed container (e.g., a motorblock) because the soil is essentially an open system. Therefore, when the water in the upper layers of the soil freezes, the water can move freely to and from the freezing front. The pressure a soil develops on freezing is the result of the surface energy between ice and water. In this paper an attempt is made to relate the maximum pressure a soil develops to the pore size distribution of a soil.

REVIEW OF THE LITERATURE

Several studies, both in the laboratory and the field, have been made on the origin and magnitude of the heaving pressure (1, 2, 9, 14, 16).

Taber (16) found that a maximum pressure of 105 psi developed on freezing a clay. Since his system developed large friction forces, he estimated a total pressure of 200 psi. More significant, however, was his observation that the pressure not only develops in an ice-water system, but is common to all growing crystals.

Heaving pressure measurements in a cylindrical sample in the laboratory were made by Balduzzi (1). The heaving pressure and the pore water pressure were measured simultaneously. He found that tension in the pore water reduced the heaving pressure.

The influence of rate of heave under fixed loads has been determined by several other researchers. Actual measurements of the force required to prevent heaving were not made in these cases. For example, Beskow (2) found that the curves of rate of heave vs surcharge were hyperbolic, the rate of heave decreasing with increasing load. He also noted that finer grained soils were less affected by surface load. Linell and Kaplar (10) conducted the same experiments. Like Beskow, they did not measure the load required to prevent heaving, but determined the relationship between rate of

Paper sponsored by Committee on Frost Action.

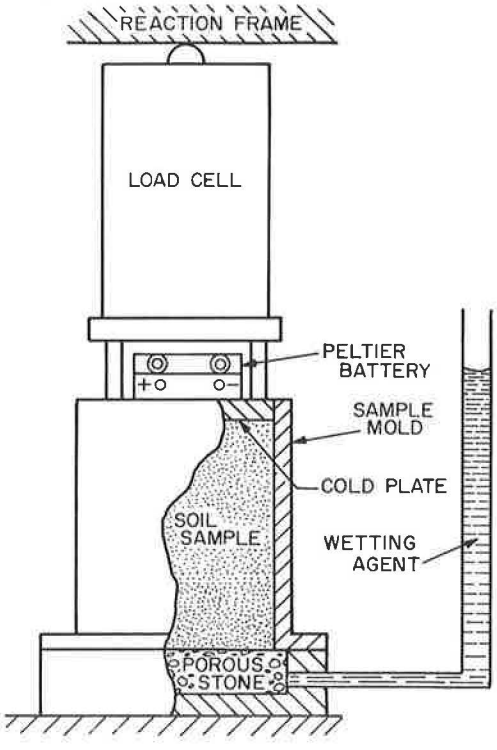

Figure 1. Schematic drawing of freezing chamber.

heave and surcharge. Penner (15) used a closed system; that is, after his samples were saturated, the water supply was cut off and the freezing was conducted without a free supply of water. By extrapolating Penner's data, a heave pressure of approximately 25 psi might be expected for powdered quartz with particle size 0.001 to 0.03 mm.

Several researchers (3, 4, 12, 14) have drawn attention to the importance of pore size in frost heaving. Miller et al. (11) showed that ice penetration into soil pores filled with water could be predicted by equilibrium thermodynamics if the geometry of the ice-water interface was taken into account.

Although pore size was known to be a governing parameter, no systematic study relating pore size and heaving pressure has so far been reported.

EXPERIMENTAL APPARATUS

From experience gained by Kaplar and others in our laboratory a test chamber was designed, as shown in Figure 1. The cylinder is a stainless steel mold, 4 in. in diameter and 5 ¼ in. in depth, tapered and coated on the inside with Teflon. A stainless steel baseplate, housing a porous stone, is attached to the bottom. The baseplate is sealed against the mold by an O-ring. A thermoelectric element is attached to the cold plate at the top of the mold. The cold plate is sealed against the mold by a U-cup. Above and bearing the thrust of the cold plate is a Baldwin load cell which in turn bears against a reaction frame.

A thermoelectric element (Pt 4 7/5, Ferroxcube Corp. of America) was used to cool the sample. The principle used is the same as that of thermocouples. When the two junctions of a thermocouple are at different temperatures, a potential difference or a current can be measured. In a thermoelectric element a potential difference is applied across the junctions of two dissimilar semiconductors and, as a result, heat is removed at one junction and dissipated at the other junction. The rate of heat removal is controlled by the current through the element (7).

The thermoelectric element used has a cooling capacity of 54 BTU/hr. For our sample this corresponds to a frost penetration of approximately 1 in./hr. The low voltage d. c. power supply for the thermoelectric element was a Sorensen Model QB68. The warm side of the thermoelectric element was cooled by circulating tap water. To minimize friction, the walls of the cylinder were given a 2° taper and coated with Teflon. Water was provided through the water inlet and the porous stone. The load was measured by Baldwin SR-4 load cells and recorded on a Leeds and Northrup Speedomax G. millivolt recorder. The recorder was calibrated with a Keithley differential voltmeter, Model 660.

Copper-constantan thermocouples were placed at 1-in. intervals of depth to obtain a temperature profile.

SAMPLE PREPARATION

The sample was wet to optimum moisture content to give maximum compaction using the modified Proctor method. The sample was de-aired and saturated with

de-aired water or, in the case of one series of tests, with benzene. The sample was then frozen from the top down. The ambient temperature was 5.5 C and the heave force was measured as discussed previously. On completion of a test, the water content vs tension curve was determined on the sample.

A very uniform and flat interface was formed on freezing; the difference in depth of penetration across the sample was less than $\frac{1}{8}$ in. Due to volume expansion, water was observed to flow out of the sample when a soil saturated with water was frozen. When a sample saturated with benzene was cooled, there was a flow of benzene into the sample, due to the contraction of benzene on solidification.

THEORETICAL

It was mentioned in the introduction that the pressure developed on freezing a saturated soil in an open system is due to the surface energy between ice and water. A better understanding of this phenomenon may be arrived at by considering the test chamber in Figure 1 filled with water with a constant head maintained in the standpipe. On freezing the water in the chamber a flat ice-water interface forms. As a result of the expansion of the water-ice phase change, some water flows out of the chamber through the porous stone; no pressure develops.

When there is saturated soil in the mold, the water is contained in pores. On freezing this system again, an ice-water interface forms, in this case at the boundary of frozen and unfrozen soil. However, this interface cannot be flat. For ice to proliferate through the soil pores, the interface has to be irregular. This causes the surface area of the interface in a porous system to be larger than that of a flat interface. An increase in surface area of an interface is always associated with an increased surface energy of the system.

For an interface of regular curvature thermodynamic equations can be written. The relation between the chemical potential of a flat interface μ_p to that of a curved interface μ_c is given by:

$$\mu_c - \mu_p = \frac{2\bar{v}_i \sigma}{r} \tag{1}$$

where

σ = surface tension,
$\bar{v}_i$ = partial molal volume, and
r = radius of interface.

Although this concept can be readily applied to liquid-vapor systems, it has been questioned if these principles also apply to solid-liquid interfaces. In this paper it is assumed that the surface tension theory applies also to solid-liquid interfaces. The conditions under which these assumptions are valid are extensively discussed by Herring and Kingery (5, 8).

Since there is a temperature gradient maintained in our system, it is also necessary to consider whether or not the usual thermodynamic variables and properties are still valid. When a steady state is obtained, the properties of the system do not change with time, but there can be an irreversible flow of heat, matter, or electricity through the system. The theory of irreversible thermodynamics postulates that for a non-equilibrium steady-state process, the equilibrium thermodynamics applies, so that Eq. 1 has been presented by several authors (4, 12, 15) in the form

$$\Delta P = \frac{2\sigma}{r} \tag{2}$$

Although ΔP should truly present a hydrostatic pressure, the one-dimensional heaving pressure has been substituted for P. Thus far there is no justification other than that it is far more convenient to use the heaving pressure than to consider the anisotropy in the pressure distribution.

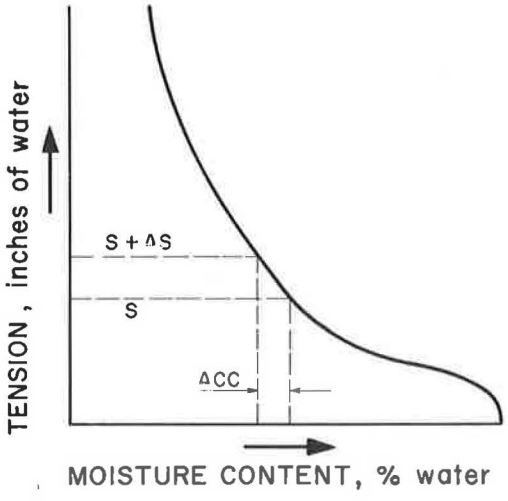

Figure 2. Typical water content vs tension curve of soil.

PORE SIZE DISTRIBUTION OF SOIL

If the radius of curvature of the interface in Eq. 2 is equated with the radius of the pores in the soil, the heaving pressure can be related to the pore size distribution of the soil. Penner (15) already pointed out that a large pore size range in the material is a drawback in making a rigorous comparison of the heaving experiment with the theory. The pore size distribution of a soil can be calculated from the water content vs tension curve of a soil. In Figure 2 a water content vs tension curve is shown. For an increment of tension, Δs, the water content changes (Δcc). This is interpreted to mean that Δcc of water is held in pore sizes defined by the equation

$$\frac{s}{2\sigma_w} < r < \frac{s + \Delta s}{2\sigma_w} \qquad (3)$$

where

r = effective pore radius,
s = tension in pore water, and
σ_w = surface tension air-water.

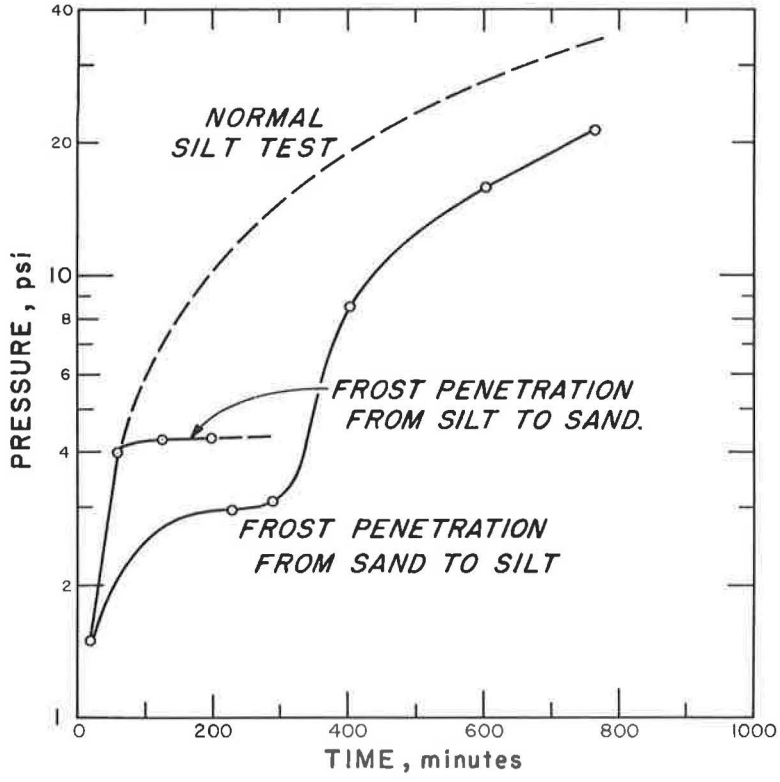

Figure 3. Pressure vs time for layered samples.

This procedure can be carried out for the entire curve so that a pore size distribution curve can be obtained. To relate the heaving pressure of a soil to the pore size distribution, a characteristic pore size will have to be determined empirically. The determination of a characteristic pore size will be discussed. Another point that needs to be discussed is the entry of ice into a pore filled with water. Once ice grows into a large pore, it will not grow all the way down because it will reach a region of higher temperature and growth will stop. An ice-water interface forms somewhere in the pore. This is different from air entry into a pore filled with water. When air entry takes place in a pore filled with water, all water is forced out of that pore. No air-water interface forms in the pore.

RESULTS AND DISCUSSION

If the pressure developed on freezing a soil is the result of the surface energy between ice and water, then this pressure should originate at the freezing front. This hypothesis was tested on a stratified sample with layers of sand and silt packed in the test chamber. Since the pores in a sandy soil are larger than in a silt soil, the pressure should increase faster when the freezing front moves from the sand to the silt. Figure 3 shows that the experiments verify the hypothesis. The movement from sand to silt shows the reverse effect.

If the pressure developed is the result of the surface energy of a solid-liquid interface in a porous system, the pressure should not be a property of the ice-water system only, but should also occur when, e. g., benzene solidifies in the system. This was verified on Richfield silt (Fig. 4). The pressure developed in the same manner for a benzene-saturated soil as for a soil saturated with water. The difference in pressure

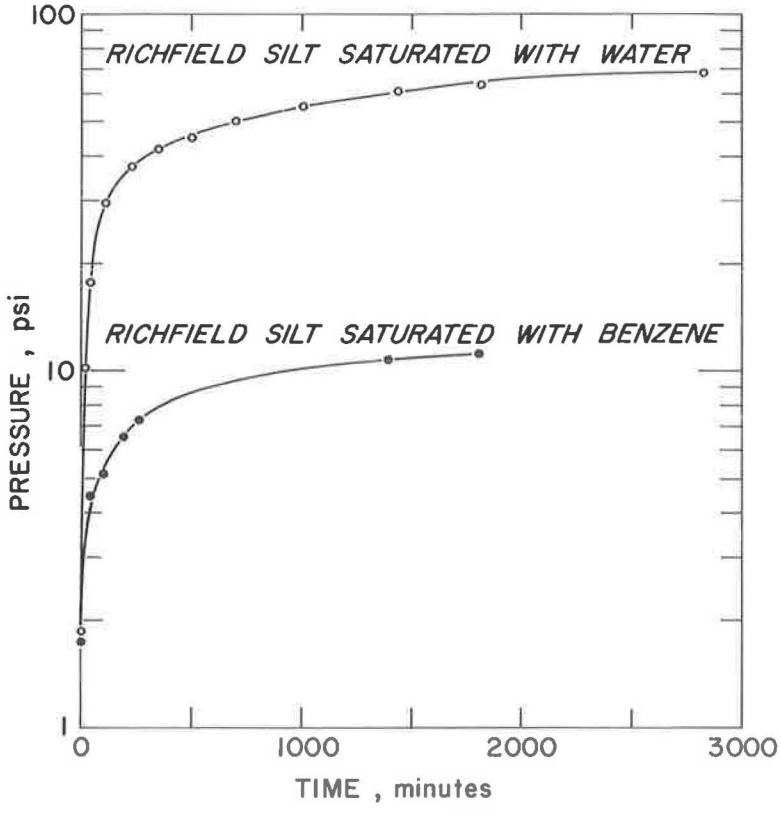

Figure 4. Pressure vs time for Richfield silt saturated with benzene.

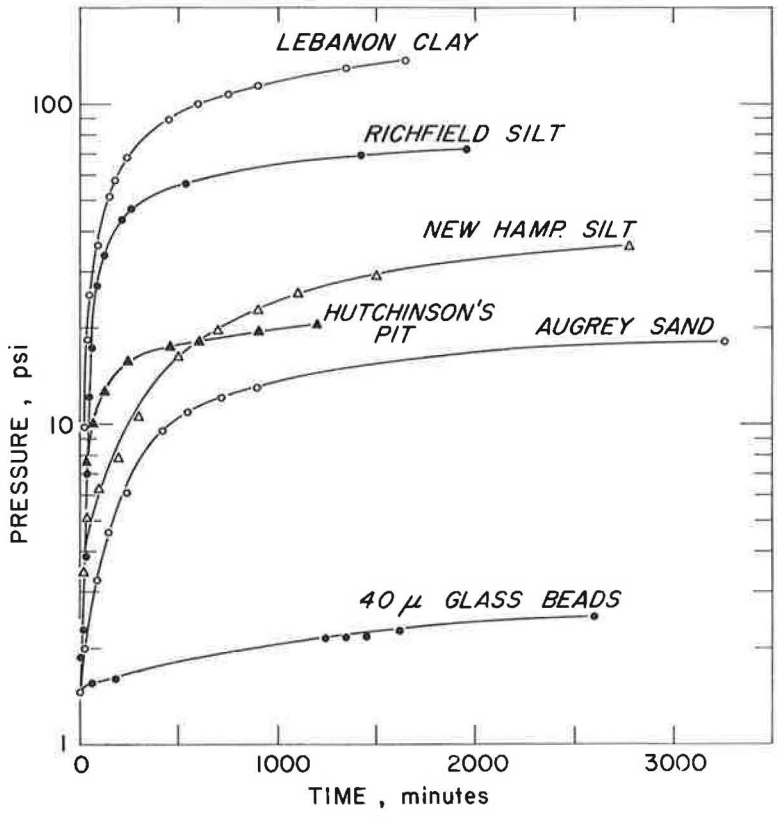

Figure 5. Pressure vs time for several soils.

is due to the different values of the surface tension of ice-water and liquid-solid benzene. This experiment has another important implication. Not all water freezes in a soil at temperatures close to 0 C. The "unfrozen water" freezes gradually at lower temperatures. It is conceivable that the pressure is due to expansion on freezing of the unfrozen water. Since benzene contracts on solidification, the pressure developed must be due to the surface energy of the liquid-solid interface.

In Figure 5, the increase in load with time is plotted for several soils. Several runs were performed on each soil. The maximum pressure that develops is reproducible to within 10 percent. This is an important observation since it means that the pressure can probably be used as a criterion to indicate the behavior of soils on freezing. The maximum pressure is developed when the position of the freezing front becomes stable in the soil. To show that the pressure cannot increase beyond a maximum value even when further penetration occurs, an initial load slightly higher than the expected maximum load was placed on the sample, and the sample was frozen. Figure 6 shows that the pressure never increases beyond the expected maximum load. The increase in pressure with time can be described by:

$$P = A\,[\,1 - \exp(-a\sqrt{t})\,] \qquad (4)$$

where

A = maximum pressure,
a = constant,
P = pressure (psi), and
t = time (min).

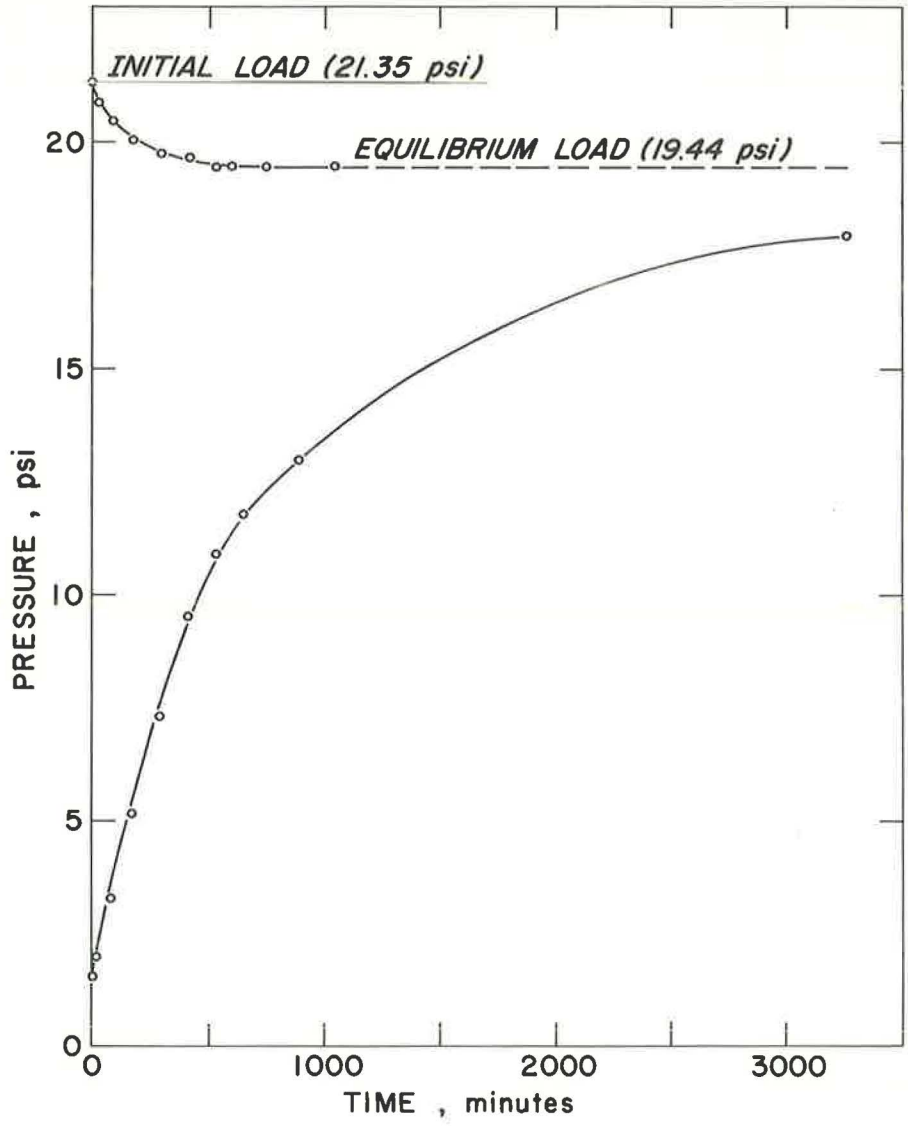

Figure 6. Pressure vs time for augrey sand with and without an initial load.

When $t \to \infty$, $\exp(-a\sqrt{t}) \to 0$, and $P \to A$. This relation can be written as:

$$\ln (A - P) = \ln A - a\sqrt{t}$$

If the maximum value is estimated from Figure 5, A_{est}, can be inserted in Eq. 4 in the form:

$$\ln (A_{est} - P) = \ln A - a\sqrt{t} \qquad (5)$$

This relation is plotted for several soils in Figure 7. This shows that Eq. 4 adequately describes the increase in pressure with time. From the intercept at time zero, ln A is obtained. If A differs from A_{est}, A and A_{est} can be made to coincide by successive

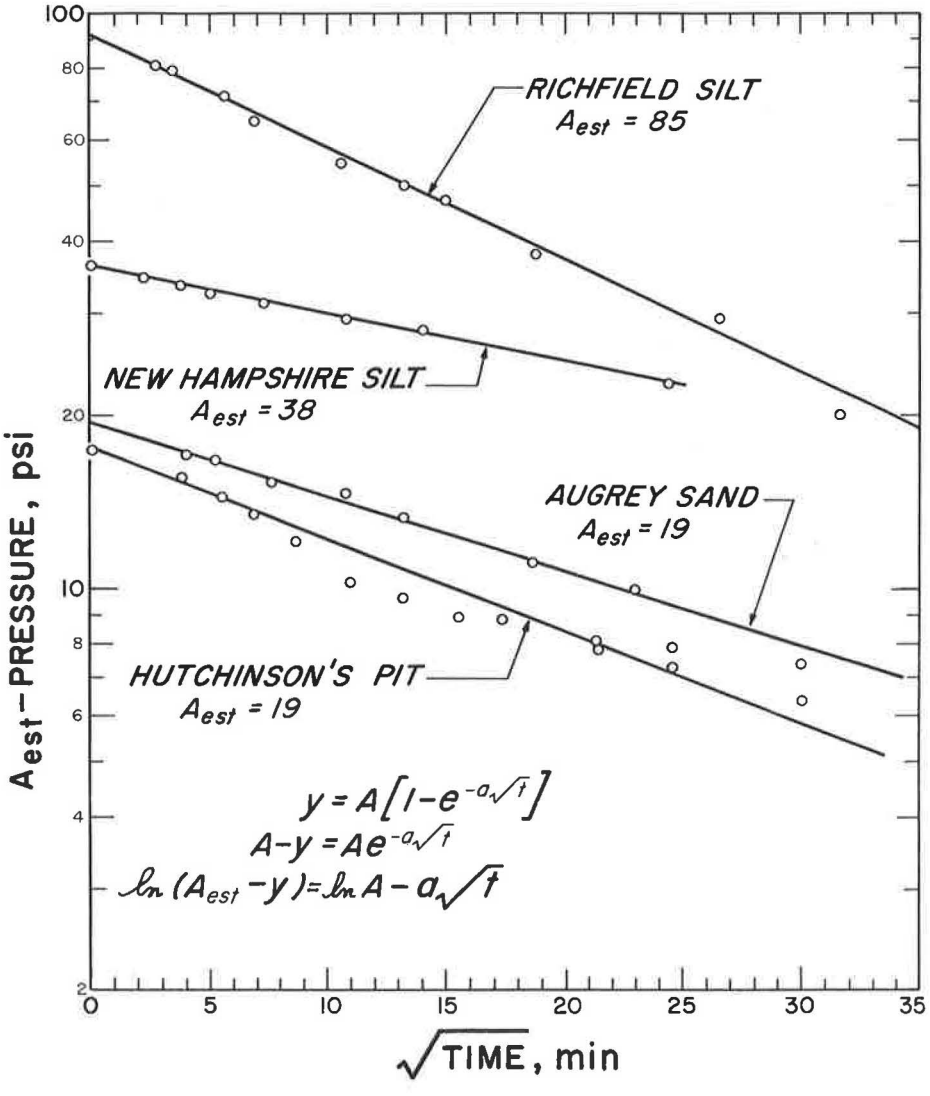

Figure 7. Difference between estimated maximum pressure and pressure at time t vs root of time.

approximations. However, it was found that near agreement was obtained on the first approximation. The maximum pressure can thus be evaluated from a 24-hr test.

In Figure 8 the percent saturation vs tension curves of the soils used are given. An empirical criterion has to be established to correlate the pressure developed with the percent saturation vs tension curve of the soil. In establishing an empirical criterion, the following reasoning was used. The maximum pressure will be developed so that the ice interface can proliferate through the smallest pores. However, this cannot be the only criterion; the number of small pores present is another. If there were only a few pores of a small size present, the freezing front could bypass these pores. The amount of water held in pores of a particular size range is given by the slope of the curves in Figure 8; the point where the slope of the line decreases rapidly is indicated. In Figure 9 the tension at this point is plotted vs the pressure developed. There is a consistent relationship between the tension at the points indicated in Figure 8 and the pressure.

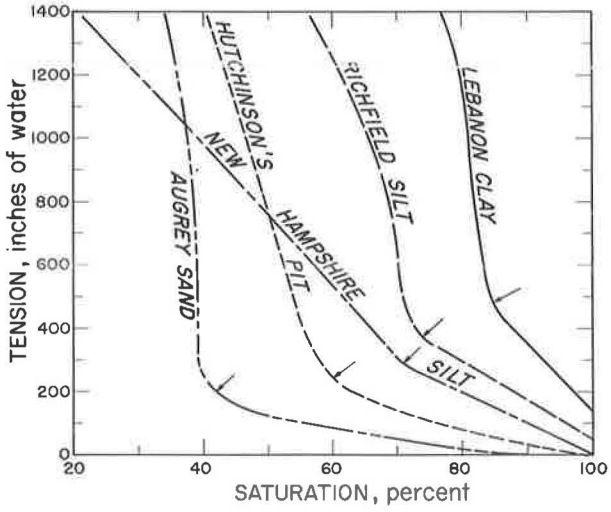

Figure 8. Percent saturation vs tension curves for several soils.

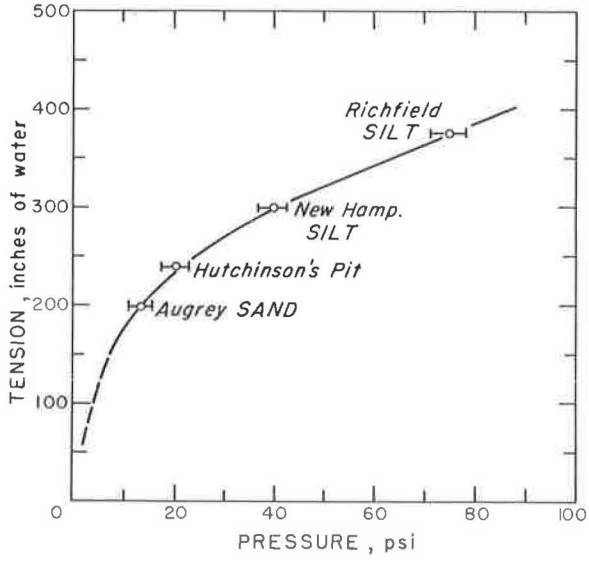

Figure 9. Pressure vs tension at points indicated in Figure 8.

CONCLUDING REMARKS

All present criteria for frost susceptibility are based on the grain size distribution of the soil. A close look at the frost-heaving process reveals that pore size is a more fundamental soil parameter than grain size. The grain size distribution is partly successful in predicting frost susceptibility because grain sizes and pore sizes are somewhat related. However, particle shape and gradation obscure the relationship between grain sizes and pore sizes. In Figure 10 the grain size distributions of the soils used are given. The Richfield silt and augrey sand have different degrees of frost susceptibility. The soils would, however, both be classified as SM in the Unified System. The maximum heaving pressure differentiates between these soils (Fig. 5)

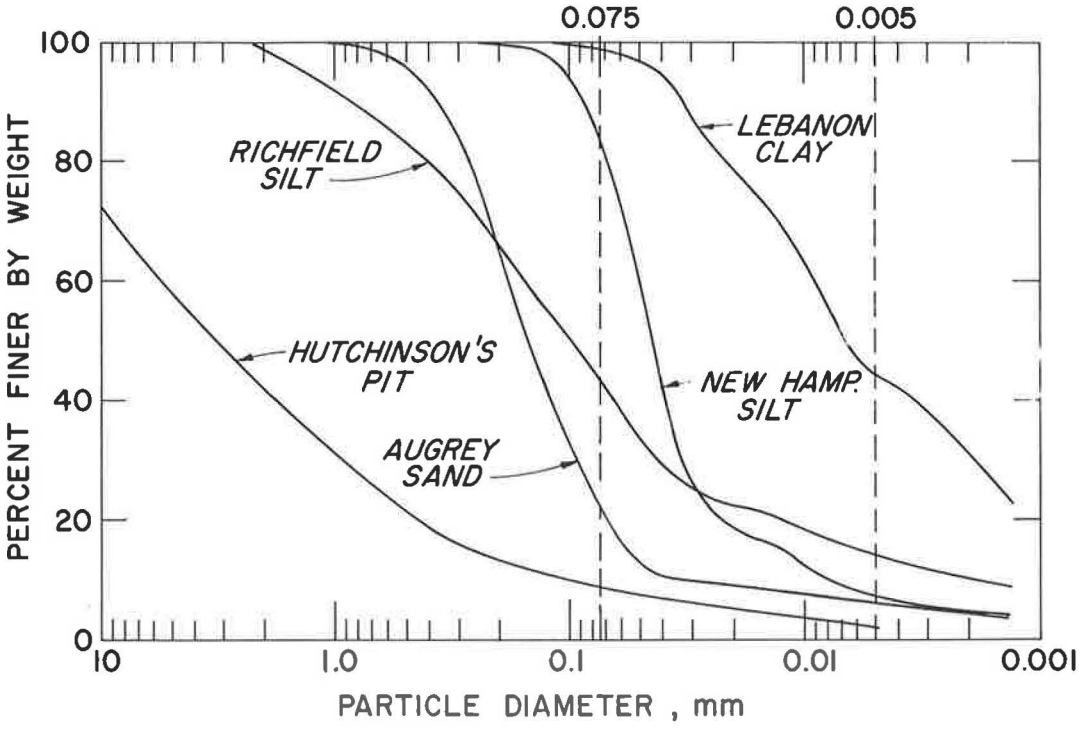

Figure 10. Grain size distributions of several soils.

and there is a consistent relation (Fig. 9) between heaving pressure and the pore size distribution of the soil. Additional research is being undertaken to test more soils and to determine if the heaving pressure provides a reliable criterion for frost susceptibility.

REFERENCES

1. Balduzzi, F. Experimental Investigation of Soil Freezing. Nat. Res. Coun., Canada, Tech. Transl. 912, 1959.
2. Beskow, G. Soil Freezing and Frost Heaving with Special Application to Roads and Railroads (transl. by J. Osterberg). Northwestern Univ. Tech. Inst., 1947.
3. Chalmers, B., and Jackson, K. A. U. S. Army Corps of Eng., Final Rept. 5745.
4. Everett, D. H. The Thermodynamics of Frost Damage to Porous Solids. Farad. Soc. Trans., p. 1541, 1961.
5. Herring, C. The Use of Classical Macroscopic Concepts in Surface Energy Problems. In Structure and Properties of Solid Surfaces. Univ. of Chicago Press, 1952.
6. Hillig, W. B. The Kinetics of Freezing of Ice in the Direction of the Basal Plane. Proc. Int. Conf. Crystal Growth, p. 350, 1958.
7. Hoekstra, P. Thermo-Electric Cooling for Frost Effect Tests. Proc. SSSA, Vol. 28, p. 716, 1964.
8. Kingery, W. D. Introduction to Ceramics. New York, John Wiley and Sons.
9. Kinoshita, S. Heave Force of Frozen Soil. Low Temperature Science, Kitami Tech. College, Ser. A. 21., 1962.
10. Linell, K. A., and Kaplar, C. W. The Factor of Soil and Material Type in Frost Action. Highway Research Board Bull. 225, pp. 81-128, 1959.

11. Miller, R. D., Baker, J. H., and Kolaian, J. H. Particle Size, Pore Water Pressure and Freezing Temperature of Ice Lenses in Soil. Trans. 7th Int. Conf. Soil Sci., Vol. 1, p. 122, 1960.
12. Miller, R. D. Phase Equilibria and Soil Freezing, Int. Conf. Permafrost, Purdue Univ., 1963.
13. Penner, E. The Nature of Frost Heaving. Int. Conf. Permafrost, Purdue Univ., 1963.
14. Penner, E. The Mechanism of Frost Heaving in Soils. Highway Research Board Bull. 225, pp. 1-22, 1959.
15. Penner, E. Pressures Developed in a Porous Granular System as a Result of Ice Segregation. Highway Research Board Spec. Rept. 40, pp. 191-199, 1958.
16. Taber, S. Frost Heaving. Jour. Geology, Vol. 37, No. 5, p. 428, 1924.

Excess Pore Pressures Which Develop During Thawing of Frozen Fine-Grained Subgrade Soils

LESLIE Y. C. YAO and BENGT B. BROMS
Respectively, Senior Engineer, Dames and Moore, New York; and Associate Professor of Civil Engineering, Cornell University

The bearing capacity of flexible pavement is generally governed by the bearing capacity of the subgrade soil which can be greatly reduced during the spring breakup period if the subgrade soil is frost susceptible. This reduction in strength is caused by an increase in water content during freezing, a decrease in soil density and incomplete dissipation of the excess pore pressures during thawing. Methods are presented by which the excess pore pressures before application of any external loads can be calculated within a subgrade during and after thawing.

•DURING FREEZING of fine-grained soils, water is drawn from the groundwater table to the freezing front. The amount of water attracted and the thickness and spacing of the resulting ice lenses that form during freezing depend mainly on rate of freezing, grain size and gradation of the subgrade soil, distance from the water table, and intensity of surcharge load (1, 2, 8, 9, 15, 18, 19).

During thawing, large amounts of excess water will be retained in the soil when the permeability of the soil is low. Several weeks may be required for full dissipation of this excess water.

The shearing strength of the subgrade soil can be greatly reduced during the spring breakup period after it has been subjected to freezing and thawing. This reduction in strength is caused by an increase in water content of the soil, a decrease in soil density, and high excess pore pressures. As a consequence, the bearing capacity of the subgrade will also be reduced and extensive damage to highway and airfield pavements may result.

The shearing strength of a subgrade generally reaches its lowest value at the beginning of the thawing period when the excess pore pressures reach a maximum. The excess pore pressures will gradually decrease with time and, consequently, the subgrade will gradually gain in strength. It is important to be able to predict this variation in shear strength and bearing capacity at any stage during the thawing period so that imposed loads (wheel or axle loads) can be maintained within safe limits.

Methods are presented by which the ultimate bearing capacity and the excess pore pressures which develop within subgrade soils can be estimated at any stage and at any depth during the thawing period.

It should be emphasized that the calculated pore pressures have not been substantiated by test data and, therefore, the limitations of the proposed method are not known. The method is presented only as a working hypothesis. Its main justification is to point out the factors which may have an important effect on the bearing capacity of subgrade soils during the thawing period.

RELATIONSHIP BETWEEN INITIAL PORE PRESSURE AND BEARING CAPACITY

The initial pore pressures will have an appreciable effect on the bearing capacity of flexible highway and airfield pavements. The difference between the maximum and minimum principal stresses at failure, $(p_1 - p_3)_f$, of a saturated subgrade soil can be

Paper sponsored by Committee on Frost Action.

expressed in terms of initial total vertical pressure p_o, the initial pore pressure u_o, the shear strength parameters c' and φ', the coefficient of lateral earth pressure at rest K_o and the pore pressure coefficient $\bar{A}_f$ (11, 17) as follows:

$$\frac{(p_1 - p_3)_f}{2} = \frac{c' \cos \varphi' + (p_o - u_o) \sin \varphi' \, [K_o + \bar{A}_f (1 - K_o)]}{1 + (2 \bar{A}_f - 1) \sin \varphi'} \tag{1}$$

For c' equal to zero, Eq. 1 becomes:

$$\frac{(p_1 - p_3)_f}{2} = \frac{(p_o - u_o) \sin \varphi \, [K_o + \bar{A}_f (1 - K_o)]}{1 + (2 \bar{A}_f - 1) \sin \varphi'} \tag{2}$$

In the derivation of Eqs. 1 and 2, it has been assumed that the soil is saturated and that no change in water content takes place during loading. If, however, an appreciable change does take place, the shear strength generally will be higher than that calculated from Eqs. 1 or 2. Thus, these equations will yield results which generally are on the safe side.

The validity of Eqs. 1 and 2 has been demonstrated mainly for remolded soils. The limitations of these equations to undisturbed soils are not known.

If the load causing failure is applied very rapidly (such as by moving traffic loads), the water content of most soils will not change appreciably. The loading rate necessary to prevent a change in water content during loading depends on the permeability and compressibility of the soil and on the boundary conditions. The permeability is the most important of these factors.

Broms (3) has proposed a method for the evaluation of the ultimate bearing capacity of flexible pavements subjected to frost action. It has been assumed in this method that a saturated soil, with a low permeability compared to the loading rate (when no or very little change in water content takes place during loading), will behave as a frictionless material with a shear strength c_u. This shear strength can be evaluated by the equation (17):

$$c_u = \tfrac{1}{2} (p_1 - p_3)_f \tag{3}$$

The corresponding net ultimate bearing capacity q_{ult}^{net}, defined as the total ultimate capacity less the overburden pressure, can then be calculated by the equation (13, 17, 20):

$$q_{ult}^{net} = c_u N_c \tag{4}$$

where N_c is a bearing capacity factor that depends on the shape and size of the loaded area as well as on the depth below the ground surface (20).

If Eqs. 3 and 4 are substituted into Eqs. 1 and 2, then:

$$q_{ult}^{net} = \frac{c' \cos \varphi' + (p_o - u_o) \sin \varphi' \, [K_o + \bar{A}_f (1 - K_o)]}{1 + (2 \bar{A}_f - 1) \sin \varphi'} N_c \tag{5}$$

When c' is equal to zero, Eq. 5 becomes:

$$q_{ult}^{net} = \frac{(p_o - u_o) \sin \varphi' \, [K_o + \bar{A}_f (1 - K_o)] \, N_c}{1 + (2 \bar{A}_f - 1) \sin \varphi'} \tag{6}$$

The parameters c', φ', K_o and $\bar{A}_f$ in Eqs. 1, 2, 5 and 6 can be evaluated experimentally. The apparent angle of internal friction φ' with respect to effective stresses has been found to be almost unaffected by freezing and thawing, whereas the apparent cohesion c' depends to a large extent on the rate of freezing, the number of freeze and thaw cycles, the overburden pressures, and the drainage conditions (4).

It can be seen from Eqs. 5 and 6 that the initial pore pressure u_o will have a large effect on the ultimate bearing capacity, especially for the case when the cohesion c' is equal to zero. The ultimate bearing capacity will, for this case, approach zero when the initial pore pressure u_o approaches the initial total overburden pressure p_o.

ASSUMPTIONS

In the analysis of the excess pore pressures which develop as a result of thawing of a frozen soil, the following assumptions will be made:

1. During thawing of an area of frozen ground, flow of the melted water will only take place toward the ground surface (before the soil has thawed completely). Therefore, regardless of the location of the original groundwater table, the water table will be temporarily raised during thawing. The groundwater table may be raised to the ground surface or to any pervious layer located within the thawed part of the soil. As a consequence, the subgrade soil becomes saturated or almost saturated during thawing. When the lateral extent of the subgrade is large compared to the thawing depth, the flow of water will be essentially one-dimensional. The assumption will be made that the subgrade soil is fully saturated and that the flow of melted water is one-dimensional.
2. During freezing of fine-grained soils, water is drawn to the freezing front from any available source and will form more or less continuous ice lenses or ice bands. When the ice lenses melt during thawing, part of the melted water will be absorbed by the soil located between the individual ice lenses and part will dissipate during the thawing process. However, if the thawing rate is high, most of the melted water will remain in the soil for a limited period of time in the form of more or less continuous water layers. The pore pressures which develop within these continuous water sheets will be equal to the total overburden pressure since complete separation of the individual soil particles will occur at each water sheet. It will be assumed that this pore pressure will remain constant until the water trapped within the water sheets is fully dissipated and the space between the different soil layers is completely closed.
3. After the free water trapped within the continuous water sheets has dissipated, a further change in water content of the soil will take place as the excess pore pressures gradually decrease. The resulting gradual change in water content will depend primarily on the compressibility of the soil. However, soils which have been subjected to one or several freeze-thaw cycles will be heavily preloaded by high negative pore pressures which develop within the soil during the freezing cycle (4). Consequently, the volume compressibility of frozen and thawed soils will be generally small except for swelling soils. Thus, the change in water content, which takes place as the soil reconsolidates during thawing, will also be small. It will be assumed in the following analysis that these volume changes can be neglected. Thus, the methods presented in this paper will be restricted to nonswelling types of soils.

The accuracy of these assumptions is not known and, therefore, field measurements are necessary before the proposed method can be used for design purposes.

INITIAL PORE PRESSURES

Thawing Depth and Rate of Thawing

The development of excess pore pressures within a soil depends on the rate of thawing and on the consolidation rate. If, for example, the thawing rate is high as compared to the consolidation rate, then high excess pore pressures will develop within the soil. These excess pore pressures can be evaluated by considering the factors affecting the rate of thawing and the consolidation rate.

The thawing rate can be calculated from the following general differential equation which governs the one-dimensional, unsteady heat flow:

$$\frac{\partial T}{\partial t} = \alpha \frac{\partial^2 T}{\partial Z^2} \qquad (7a)$$

where

Z = depth below ground surface,
t = time,
T = temperature at time t and depth Z, and
α = thermal diffusivity as defined by:

$$\alpha = \frac{K}{c\rho} \tag{7b}$$

where

K = thermal conductivity of the material,
c = specific heat of the material, and
ρ = density of the material.

Several solutions to Eq. 7a are available. Jumikis (10) has presented one which relates frost penetration depth or the thawing depth with the thermal properties of the soil. According to Jumikis (10), the thawing depth Z_o can be determined from the equation:

$$Z_o = \sqrt{\frac{2K_1 (T_s - T_f)\, t}{Q_L \gamma_w n}} \tag{8a}$$

where

K_1 = thermal conductivity of thawed soil,
Q_L = latent heat of fusion,
γ_w = unit weight of water,
n = porosity,
T_s = surface temperature, and
T_f = freezing temperature.

Eq. 8a can be rewritten as:

$$Z_o = m\sqrt{t} \tag{8b}$$

if:

$$m = \sqrt{\frac{2K_1 (T_s - T_f)}{Q_L \gamma_w n}} \tag{8c}$$

It can be seen from Eq. 8b that the depth of thawing varies as the square root of time.

The rate of thawing equal to dZ_o/dt can then be determined from the equation:

$$\frac{dZ_o}{dt} = \frac{m}{2\sqrt{t}} \tag{8d}$$

In the derivation of Eq. 8a it has been assumed that the latent heat of fusion is the only heat conducted during thawing or freezing to or from a point within a mass of soil. The amount of heat generated or consumed by a change of temperature above or below the freezing point has been neglected. The resulting inaccuracy depends on the surface temperature, the temperature in soil, water content and thermal properties of the solids. Calculations (10) have indicated that the error in thawing depths as determined by Eq. 8a is usually less than 5 percent. The amount of heat transported by the upward flow of water during thawing has also been neglected. Calculations by the authors have indicated that this heat flow is small and has no signficant effect (less than 1 percent) on the calculated thawing depth.

Eqs. 8a and 8b can be solved for the case when the quantity m is constant, that is, when the thermal conductivity of the thawed soil, the latent heat of fusion, the porosity, the surface temperature and the freezing temperature are all constant.

Excess Pore Water During Thawing

Shown in Figure 1 is a section through a typical highway pavement consisting of a wearing course, a base course and a subgrade. During thawing and the subsequent reconsolidation of the subgrade soil, its water content will decrease from w_o to w, where w_o and w are the water contents of the frozen and fully reconsolidated soil, respectively. When the subgrade is fully saturated, the unit volume decrease dV/V caused by consolidation of the soil after thawing will be equal to:

$$\frac{dV}{V} = \frac{(w_o - w)}{w_o + 1/G_s} \tag{9}$$

where G_s is the specific weight of the solid material. The unit volume change dV/V is equal to the volume of excess water expelled from the soil during thawing and the subsequent consolidation.

In addition to the volume change dV/V which is caused by a change in water content after thawing, a volume change takes place during thawing without any change in water content due to the difference in density between ice and water. This volume change does not affect the thawing rate since the transfer of heat takes place through the thawed soil.

When the depth of thawing increases from Z_o to $(Z_o + dZ_o)$, the volume of excess melted water dQ will be equal to:

$$dQ = \frac{dZ_o A\,(w_o - w)}{w_o + 1/G_s} \tag{10}$$

The rate dQ/dt by which the excess water is freed during thawing can be calculated from Eq. 10 as:

$$\frac{dQ}{dt} = \frac{dZ_o}{dt} \cdot \frac{A\,(w_o - w)}{w_o + 1/G_s} \tag{11}$$

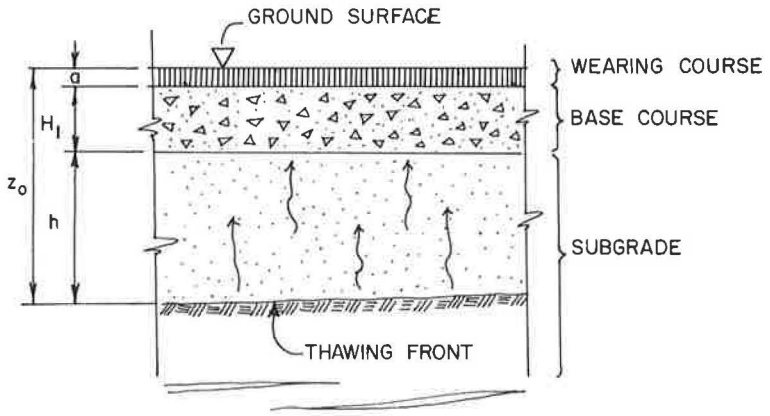

Figure 1. Cross-section through highway pavement.

The quantity dZ_o/dt is equal to the thawing rate, which is governed by Eq. 8d. Eq. 11 can then be rewritten as:

$$\frac{dQ}{dt} = \frac{mA\ (w_o - w)}{2\sqrt{t}\ (w_o + 1/G_s)} \tag{12a}$$

or

$$\frac{dQ}{dt} = \frac{m^2A\ (w_o - w)}{2Z_o\ (w_o + 1/G_s)} \tag{12b}$$

Dissipation of Excess Pore Pressures

The thawing rate may in some cases be higher than the flow rate. When this occurs, layers or sheets of water will be occupying the locations of the former ice lens and the individual soil particles will be totally separated by these water sheets as shown in Figure 2. In this case the thawed pore water will carry the weight of the overlying soil. The resulting excess pore pressure u_{excess} will be equal to the difference between the total pore pressure u and the static (e) pore pressure u_o as defined by the equation:

$$u_{excess} = u - u_o \tag{13}$$

The static pore pressure is defined as the pore pressure when no flow of water takes place through the soil.

The excess pore pressure creates a hydraulic gradient which causes the excess pore water to flow upwards. The resulting hydraulic gradient i is equal to:

$$i = \frac{u_{excess}}{h\ \gamma_w} \tag{14}$$

where h is the length of the flow path (equal to the depth of the thawed subgrade soil for the case shown in Figure 1) and γ_w is the unit weight of water. The velocity v of this flow is governed by the Darcy law:

$$v = ki \tag{15}$$

where k is the permeability of thawed soil.

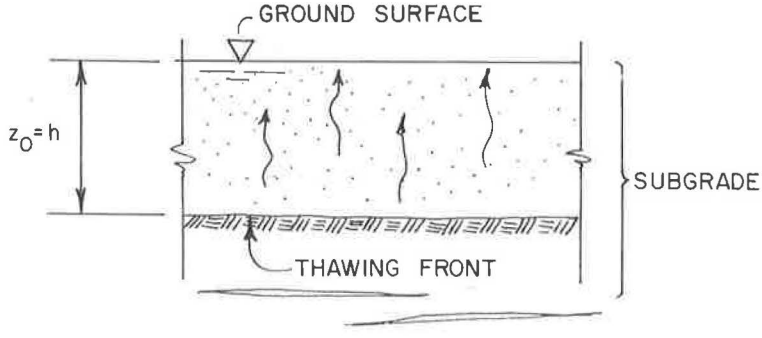

FIGURE 2 – CONDITIONS DURING THAWING (CASE 1)

Figure 2. Conditions during thawing (case 1).

The corresponding flow rate q is proportional to the available area A. Then:

$$q = Aki \tag{16}$$

If the rate of thawing is higher than the corresponding flow rate, excess pore water will accumulate in the soil and a "quick" condition will be created. This condition occurs when the seepage pressure in the soil is equal to the effective pressure, i.e., when the effective pressure becomes zero. Under this condition, the shear strength of the soil will decrease to zero in the case when the cohesion c' of the soil is equal to zero, as can be seen from Eq. 2.

Critical Depth

The thawing rate decreases with increasing thawing depth (Eq. 8d) while the flow rate remains constant. A quick condition occurs in the subgrade in the beginning of the thawing period when the thawing depth is small and the rate of thawing is high. The depth at which the behavior of the soil converts from a quick to a nonquick condition is defined as the critical depth. At the critical depth, Z_{cr}, the rate of excess water liberation (Eq. 12b) is exactly equal to the rate of excess water dissipation (Eq. 16). This occurs when:

$$\frac{m^2 (w_o - w)}{2Z_{cr} (w_o + 1/G_s)} = ki \tag{17}$$

The critical depth Z_{cr} can then be calculated from Eq. 17 as:

$$Z_{cr} = \frac{m^2 (w_o - w)}{2ki (w_o + 1/G_s)} \tag{18}$$

Within the critical region (where the soil is in a quick condition), the excess pore pressure will be independent of the dissipation rate and the rate of thawing (Eq. 18), and the excess pore pressure will depend only on the depth below the ground surface and the submerged unit weight of the soil (Eq. 13).

Subcritical conditions will occur below the critical depth. Within this region, the excess pore pressures will depend on the rate of thawing, the depth below the ground surface, the porosity and the permeability of the thawed soil. The general equation governing the excess pore pressures within this region can be determined by substituting Eq. 14 into Eq. 17. Then for the subcritical region:

$$u_{excess} = \frac{m^2 h \gamma_w (w_o - w)}{2kZ_o (w_o + 1/G_s)} \tag{19}$$

This equation will be used in the following to calculate excess pore pressures. In the derivation of Eq. 19 it has been assumed that the compressibility of the soil and the volume changes which take place due to a change in effective pressure are small and can be neglected as discussed previously. It should also be emphasized that the derived equations have not been checked by test data.

EXAMPLES

The excess pore pressures which develop during thawing within a subgrade have been investigated for three cases. It will be shown that the excess pore pressures frequently will be high and may approach the total overburden pressure.

TABLE 1
ASSUMED PROPERTIES OF SUBGRADE SOIL

Property	Value	
	Immediately After Thawing	Completion of Thawing
Water content (%)	24.0	20.0
Specific gravity of solids	2.77	2.77
Coefficient of permeability (ft/hr)	3.0×10^{-4}	-
Thermal conductivity (Btu/ft-hr-°F)	1.07	-

Case 1

In Figure 2 is shown the drainage conditions during thawing of a subgrade soil. It has been assumed in this case that the groundwater table has been raised temporarily to the ground surface. The assumed physical properties of the subgrade are listed in Table 1. Thus, it has been assumed that the water content of the soil immediately after thawing is 24.0 percent and that this water content is decreased to 20 percent after dissipation of the excess water several weeks after completion of the thawing process. In the calculations of critical depth and excess pore pressures, it has been assumed that the surface temperature has been suddenly increased to 60 F and that the average temperature of the frozen soil is 32 F.

The rate of thawing as calculated from Eq. 8b is shown in Figure 3. It can be seen that the rate of thawing decreases rapidly with increasing depth. For example, it will take 45 hr for the thaw line to reach a depth of 0.87 ft below the ground surface, and 181 hr for it to reach 1.75 ft.

The critical depth depends on the excess pore pressures within the soil and on the resulting hydraulic gradient. (At the critical depth, the excess pore pressures within the soil will be equal to the total overburden pressure.) The excess pore pressure u_{excess} within the critical depth can be determined from Eq. 13 as:

$$u_{excess} = h\gamma_{sat} - h\gamma_w = h\gamma_{sub} \tag{20}$$

where γ_{sub} is the submerged unit weight of the subgrade soil.

For this condition, the hydraulic gradient i will be equal to:

$$i = \frac{\gamma_{sub}}{\gamma_w} \tag{21}$$

The critical depth Z_{cr} (Eq. 18) can then be calculated as:

$$Z_{cr} = \frac{m^2 (w_o - w) \gamma_w}{2k (w_o + 1/G_s) \gamma_{sub}} \tag{22}$$

The critical depth will be 1.75 ft for the soil with the physical properties shown in Table 1. The time required for the thawing front to reach this depth is 181 hr or 7.6

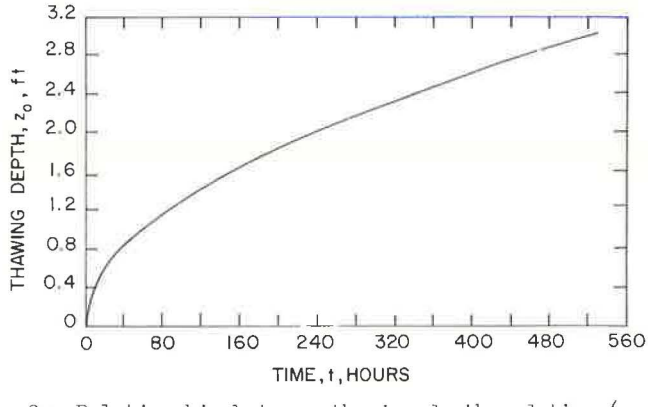

Figure 3. Relationship between thawing depth and time (case 1).

days. Thus, for 7.6 days, very high excess pore pressures will be present within the subgrade located above the thawing front and, as a result, the effective stress within the soil located above the thawing front will be reduced to zero. The corresponding hydraulic gradient is 1.063.

It should, however, be noticed from Eq. 22 that the critical depth is very sensitive to small changes of the permeability. If, for example, the permeability of the soil is equal to 1.0×10^{-4} ft/hr instead of 3.0×10^{-4} ft/hr, the critical depth will be 5.25 ft and the time required for the thaw line to reach this depth will be 68 days.

The excess pore pressure for the subcritical condition below the critical depth Z_{cr} can be determined from Eq. 19. For case 1, the depth Z_o is equal to h. For this condition:

$$u_{excess} = \frac{m^2 \gamma_w (w_o - w)}{2k (w_o + 1/G_s)} \tag{23}$$

It can be seen from Eq. 23 that the excess pore pressure u_{excess} is constant and independent of depth. This excess pore pressure will be equal to 116.0 psf for the assumed properties of the subgrade soil (Table 1).

The corresponding hydraulic gradient within the subcritical region, below the critical depth, can be calculated from Eq. 14. This hydraulic gradient is equal to:

$$i = 1.86/Z_o \tag{24}$$

The hydraulic gradient and the resulting flow rate will remain constant as thawing takes place from the ground surface and down to the critical depth of 1.75 ft below the ground surface (Eq. 21). The pore pressure will remain constant within the soil and will be equal to the total overburden pressure as long as the thaw line is located above the critical depth, the pore pressures will decrease with increasing depth of thawing, and the hydraulic gradient and the flow rate will decrease in proportion to the thawing depth, as can be seen from Eq. 24.

The corresponding distribution of excess pore pressures is shown in Figure 4 by relationships (a) through (d). Relationship (a) illustrates the pore pressure distribution when the thawing proceeds from the ground surface down to the critical depth of 1.75 ft. Relationships (b), (c) and (d) show the distribution of excess pore pressures when the thaw line has proceeded down to a depth of 2.2, 2.6, and 3.0 ft, respectively, below the ground surface. The thaw line will reach these depths 287, 400, and 535 hr, respectively, after the beginning of the thawing period. When the thaw line has reached the depth of 3.50 ft, the excess pore pressure above the critical depth will decrease

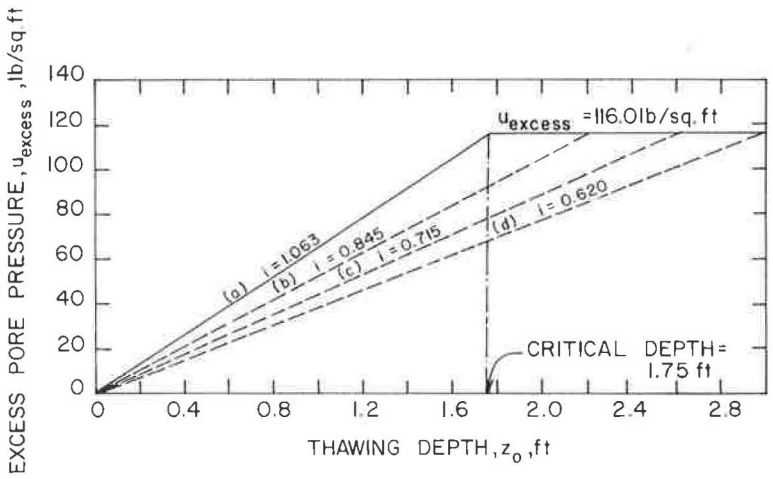

Figure 4. Relationship between excess pore pressure and thawing depth (case 1).

TABLE 2

ASSUMED PROPERTIES OF BASE COURSE MATERIAL

Property	Value
Water content (%)	12.0
Porosity	0.238
Specific gravity of solids	2.60
Thermal conductivity (Btu/ft-hr-°F)	1.80

to half its initial maximum value and the soil will have regained a large portion of its initial strength.

Case 2

In Figure 5 is shown the boundary conditions of a subgrade soil when groundwater table is not raised all the way to the ground surface. In this case, drainage takes place through a base course consisting of coarse material with a high permeability.

The same properties of the subgrade material have been chosen as for case 1 (Table 1). The assumed properties of the base and wearing course materials are given in Table 2.

The base course material located above the water table has been assumed to have a lower water content than the subgrade soil. Furthermore, it has been assumed that the thermal properties and the thawing rates are different for the two materials. (The thawing rate is frequently higher for the base course than for the subgrade material.) The equations governing the thawing rate are not continuous in this case. However, these equations can be simplified if the thickness of the base course soil is converted into an equivalent subgrade thickness. Then the base course can be treated as part of the subgrade.

Equivalent Thickness. —From Eq. 8b it can be seen that the thawing rate depends only on the parameter m which depends on the thermal properties of the soil. Therefore, the thickness of the base course can be converted into an equivalent thickness H of subgrade soil by the following relationship:

$$H = \frac{mH_1}{m_1} \tag{25}$$

where

m = parameter depending on thermal properties of subgrade soil (Eq. 8c),
m_1 = parameter depending on thermal properties of base course material (Eq. 8c), and
H_1 = thickness of base course (Fig. 5).

The pavement itself will have little effect on the thawing depth since its moisture content is generally low. From Eqs. 8c and 25, the equivalent thickness H of the base course material (Table 2) can be calculated as $0.596\ H_1$.

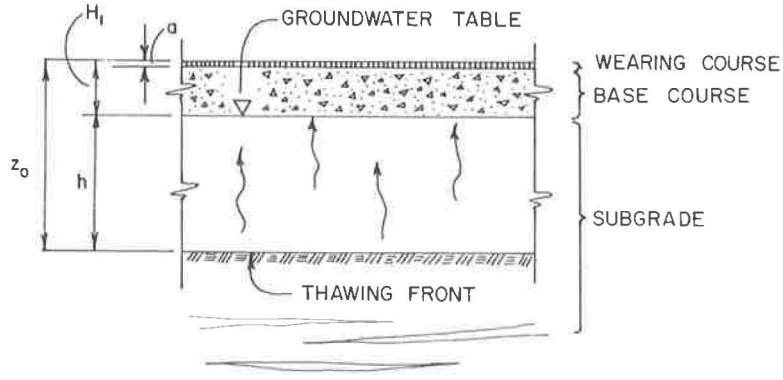

Figure 5. Cross-section through highway pavement (case 2).

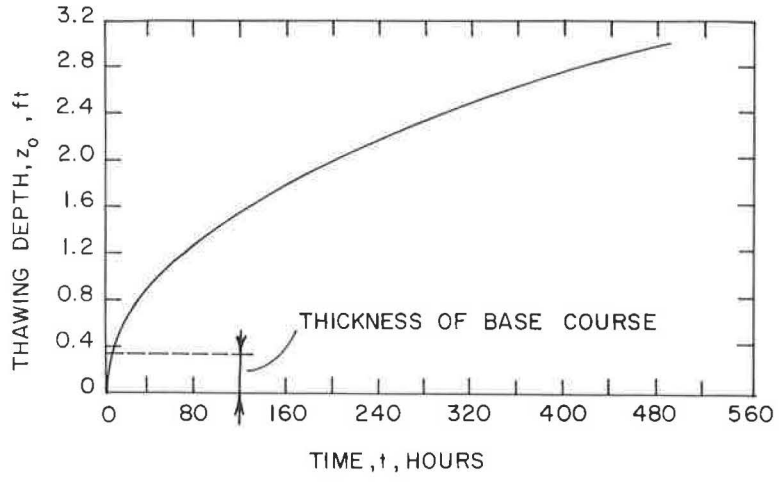

Figure 6. Relationship between thawing depth and time (case 2).

The relationship between depth of thawing and time, calculated from Eqs. 8b and 25, is shown in Figure 6. It can be seen that only a short time period is required for the thaw line to penetrate through the base course.

The critical depth can then be calculated from Eq. 18 as:

$$Z_{cr} = \frac{m^2 (w_o - w)}{2k (w_o + 1/G_s)} \left[\frac{1}{\frac{a\gamma_p}{h\gamma_w} + \frac{H_1 (\gamma_1)_{sat}}{h\gamma_w} + \frac{(\gamma_2)_{sub}}{\gamma_w}} \right] \tag{26}$$

In this equation, a and γ_p are the thickness and unit weight, respectively, of the wearing course, and H_1 and $(\gamma_1)_{sat}$ are the thickness and saturated unit weight, respectively, of the base course material. It should be noted in Eq. 26 that Z_{cr} is the equivalent critical depth. This depth is equal to $(H + h_{cr})$.

It has been assumed in this case that the thickness of wearing course, a, is negligible and the thickness of base course, H_1, is 4.0 in. The solution to Eq. 26 yields the two critical depths, 0.216 and 0.640 ft. These two depths correspond to the actual depths of 0.549 and 0.973 ft. The two solutions of Eq. 26 indicate that critical or quick conditions will exist within the subgrade soil when the thaw line is located between 0.549 and 0.973 ft below the ground surface. For this location of the frost line, the excess pore pressures will be equal to the total overburden pressure. These results are reasonable because at shallow thawing depths, the hydraulic gradient will be high due to the imposed surcharge weight (the weight of the base and wearing courses) and a relatively short time will be required for the excess water to dissipate. The excess pore pressures will be governed by the thawing rate.

The excess pore pressure u_{excess} within critical region can be determined from Eqs. 13 and 14 as:

$$u_{excess} = a\gamma_p + H_1 (\gamma_1)_{sat} + h (\gamma_2)_{sub} \tag{27}$$

The corresponding hydraulic gradient as calculated from Eqs. 13 and 14 is equal to:

$$i = \frac{a\gamma_p}{h\gamma_w} + \frac{H_1 (\gamma_1)_{sat}}{h\gamma_w} + \frac{(\gamma_2)_{sub}}{\gamma_w} \tag{28}$$

Eq. 28 is only valid at the boundaries of the critical region. Within the critical region the hydraulic gradient will be constant as long as separation between the individual soil particles occurs.

It can be seen from Eqs. 21 and 28 that the hydraulic gradient when the water table is located at some depth below the ground surface is much greater than that for the case when the water table is located at the ground surface.

The excess pore pressure for subcritical conditions (Eq. 19) is equal to:

$$u_{excess} = \frac{m^2 (w_o - w) \gamma_w h}{2k (w_o + 1/G_s) (H + h)} \tag{29}$$

For the specific case when h >>H, then:

$$u_{excess} = \frac{m^2 (w_o - w) \gamma_w}{2k (w_o + 1/G_s)} \tag{30}$$

It can be seen from Eq. 30 that for large values of h, the excess pore pressure approaches a constant value. This constant value is the same as that for case 1 when the water table is located at the ground surface (Eq. 23).

The relationships between the thawing depth and time as determined from Eq. 8a are shown in Figure 6. The relationships between the excess pore pressures, hydraulic gradients and depth of thawing are shown in Figure 7. Relationships (a) through (f) show the distribution of excess pore pressures within the subgrade as the thaw line proceeds through the subgrade down to a depth of 2.93 ft below the pavement surface. Relationship (b) indicates, for example, the excess pore pressure distribution when the thaw line has reached a depth of 1.33 ft below the ground surface. The corresponding hydraulic gradient is equal to 1.55 and the excess pore pressure at a depth of 1.2 ft below the ground surface is 84.0 psf. As the thaw line proceeds from 0.549 to 0.973 ft (critical region), the pore pressure at the thaw line will be equal to the total overburden pressure. From this value, the resulting excess pore pressures can be determined by assuming that the hydraulic gradient is constant throughout the thawed portion of the subgrade. In the calculations of the excess pore pressures shown in Figure 7, it has been assumed that the soil located above the thaw line is incompressible. It is believed that the resulting error will be small.

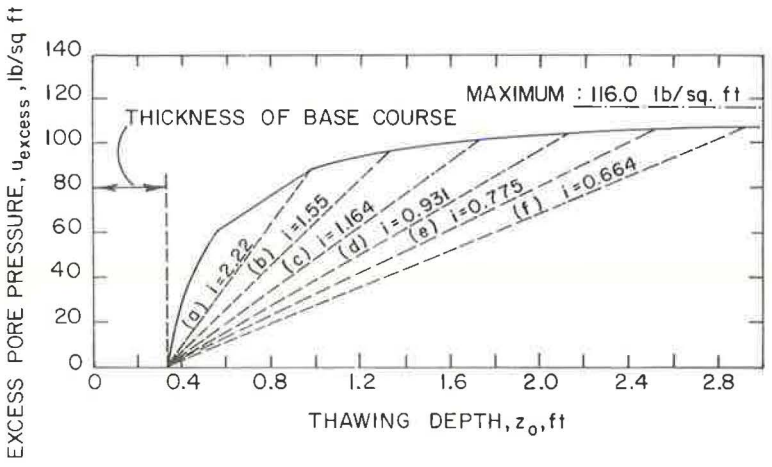

Figure 7. Relationship between excess pore pressure and thawing depth (case 2).

Effect on Ultimate Bearing Capacity. —The ultimate bearing capacity is affected by the initial excess pressures (Eqs. 5 and 6). This excess pore pressure (caused by incomplete dissipation) affects the initial effective pressures in the soil. The effect of initial pore pressure on the bearing capacity of a flexible pavement has been investigated for the subgrade shown in Figure 5. It has been assumed that the average condition in the subgrade is represented by an element located at a depth of 2.0 ft below the ground surface. The time required for the thaw line to reach this depth is 200 hr (Fig. 6). The corresponding excess pore pressure u_{excess} when the thaw line has just reached this depth is equal to 104 psf (Fig. 7). When the thaw line reaches a depth of 2.5 ft (after 325 hr), the excess pore pressure at a depth of 2.0 ft is 80 psf. Thus, at the depth of 2.0 ft, the excess pore pressures will decrease during this time by 24 psf. Similarly, when thawing depth reaches 2.9 ft, the excess pore pressure at a depth of 2.0 ft will be equal to 70 psf.

If it is assumed that the cohesive strength c' is equal to zero, and that the parameters φ', $\bar{A}_f$, K_o and N_c remain constant during thawing, the ultimate bearing capacity will be proportional to the initial effective pressure $\bar{p}_o$. For the conditions shown in Figure 5, the initial effective pressure at a depth of 2.0 ft below the ground surface will be equal to 53, 77 and 87 psf after 200, 325 and 450 hr of thawing. Thus, the bearing capacity of a subgrade soil during thawing will depend on time. After 450 hr of thawing, the bearing capacity will be 1.64 (87/53) times the bearing capacity after 200 hr of thawing. The bearing capacity of a subgrade soil will reach a minimum at the beginning of the spring breakup period and will regain slowly its original strength as the initial excess pore pressures dissipate.

Case 3

In this example, the thickness of the pavement, a, and the thickness of the base course, H_1, are each assumed to be equal to 4.0 in. The unit weight of the wearing course material has been taken as 150 pcf and its moisture content has been assumed to be small. The assumed properties of the base course and of the subgrade are shown in Tables 1 and 2.

The critical depth is governed by Eq. 26 and no real solution exists to this equation. This indicates that critical conditions will not exist within the subgrade during thawing.

The relationship between the depth of thawing and time is shown in Figure 8. It can be seen that only a very short time will be required for the thaw line to penetrate through the pavement because of its negligible latent heat of fusion. The thaw line will have penetrated to a depth of 2.49 ft after 240 hr or 10 days of thawing.

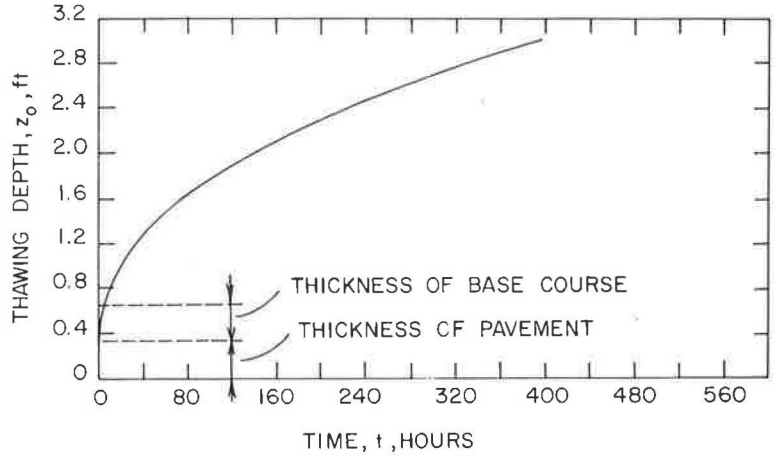

Figure 8. Relationship between thawing depth and time (case 3).

The corresponding excess pore pressures and the resulting hydraulic gradient can be computed from Eqs. 14 and 29 and are plotted in Figure 9. It can be seen that no excess pore pressures will exist within the base course or subgrade until the thaw line has penetrated through the base course. As the thaw line progresses through the subgrade, excess pore pressures will build up rapidly. The maximum pore pressure, which occurs at the thaw line, will increase with increasing depth of thawing. For example, the maximum excess pore pressure is equal to 85 psf at a depth of 1.2 ft below the ground surface. This maximum will occur 32 hr after the beginning of the thawing period and the excess pore pressure will decrease rapidly as the thawing depth increases.

DRAINAGE AND CONSOLIDATION AFTER COMPLETION OF THAWING

The equations developed in preceding sections governing the buildup and dissipation of pore pressures apply only when continuous thawing of the subgrade soil takes place and before complete thawing of the subgrade has occurred. As pointed out earlier, the water table will be temporarily raised during thawing and flow of water will only take place in the upward direction. (The soil located below the thaw line is still frozen.) However, when the soil is completely thawed, the original water table will govern the pore pressure distribution in the soil. The flow of water will be reversed and will change from that of seepage to that of drainage.

The effects of a sudden lowering of the groundwater table as a result of complete thawing on the dissipation of excess pore pressures after completion of thawing is illustrated by the following example. A cross-section through a subgrade soil is shown in Figure 10. It has been assumed that the water table is located during thawing at the ground surface while after completion of thawing, the permanent water table is located at the distance H_a below the ground surface. (The location of the permanent groundwater table is frequently governed by a stratum with a high permeability. This stratum may be located at some distance below the depth of maximum frost penetration.)

Consider first a soil element located at a distance Z_1 below the ground surface. Z_1 is assumed to be smaller than H_a. Before completion of the thawing process, the static pore pressure at Z_1 will be equal to $\gamma_w Z_1$. If the distance $(H_a - Z_1)$ is less than the height of capillary rise for the subgrade soil, the static pore pressure at Z_1 after completion of drainage will be equal to $-(H_a - Z_1)\ \gamma_w$. The increase in excess pore

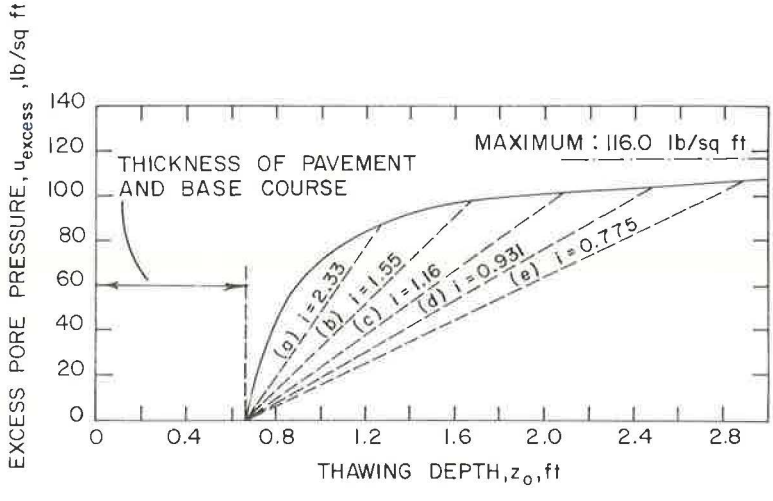

Figure 9. Relationship between excess pore pressure and thawing depth (case 3).

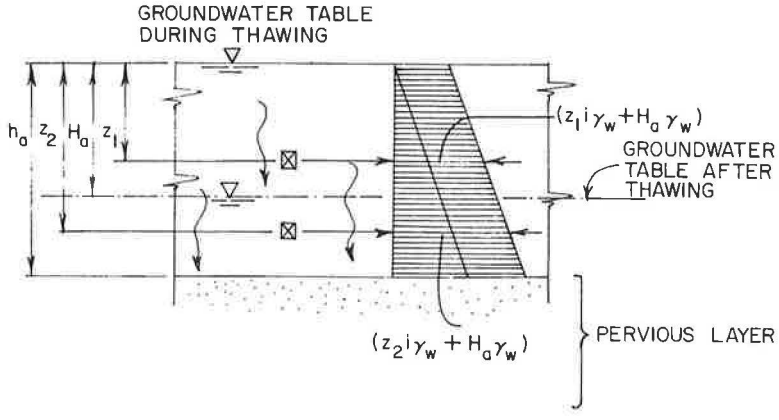

Figure 10. Distribution of excess pore pressure.

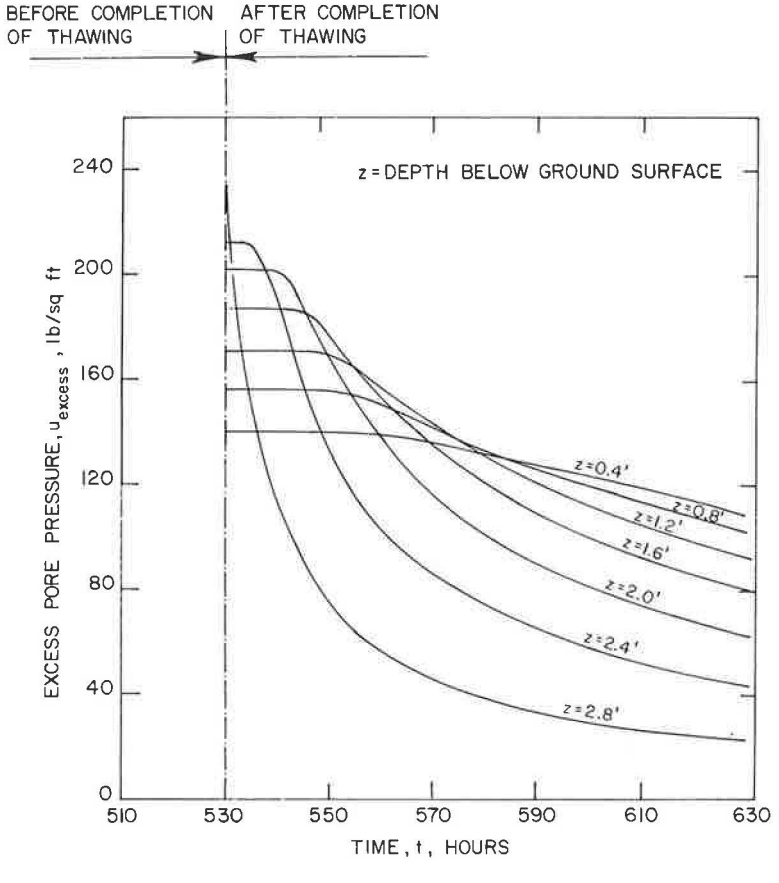

Figure 11. Dissipation of excess pore pressure.

pressure at the completion of thawing will be equal to the difference in static pore pressures before and after completion of thawing. This increase is equal to:

$$\Delta u_{excess} = Z_1 \gamma_w + (H_a - Z_1)\ \gamma_w = H_a \gamma_w \tag{31a}$$

Consider next a soil element located a distance Z_2 below the ground surface where Z_2 is larger than H. Before drainage, the static pore pressure at a distance Z_2 from the surface will be equal to $Z_2 \gamma_w$. The static pore pressure at the same level after completion of thawing will be equal to $(Z_2 - H)\ \gamma_w$. Therefore, the resulting change in excess pore pressure is equal to:

$$\Delta u_{excess} = Z_2 \gamma_w - (Z_2 - H_a)\ \gamma_w = H_a \gamma_w \tag{31b}$$

From these two examples it can be seen that the change in excess pore pressure during completion of thawing is independent of depth and is equal to $H_a\ \gamma_w$. It should be pointed out, however, that the total pressure is not changed at completion of thawing because no additional load is imposed.

The total excess pore pressure will then be equal to the sum of the initial excess pore pressure before completion of thawing and increase of excess pore pressure which occurs at completion of thawing.

The distribution of excess pore pressures during thawing has been discussed in the previous section. This excess pore pressure can be calculated if the corresponding hydraulic gradient is known. At the depth Z, the excess pore pressure during thawing is equal to $iZ\ \gamma_w$. The total excess pore pressure after completion of thawing can then be evaluated as:

$$u_{excess} = iZ\gamma_w + H_a \gamma_w \tag{32}$$

The dissipation of this excess pore pressure can be calculated by the Terzaghi consolidation theory (20). A numerical method proposed by Gibson and Lumb (7) utilizing this theory permits the determination of the excess pore pressure at any given location and at any given time.

The dissipation of excess pore pressure has been calculated for the soil conditions assumed for case 1 (Fig. 2). It has been assumed that h_a and H_a are 3.0 and 2.0 ft, respectively; that a pervious layer is located 3.0 ft below the ground surface and that no excess pore pressure exists within this pervious stratum at any time.

It can be seen from Figure 4 that the excess pore pressure during thawing is equal to 116.0 psf at the thawing front and that this pore pressure is independent of the depth of thawing. The corresponding hydraulic gradient within the thawed soil just as the thawing front reaches the depth of maximum frost penetration after 530 hr is equal to 0.620. The resulting excess pore pressures can then be calculated from Eq. 23. The dissipation of this excess pore pressure has been calculated by the numerical method mentioned previously. The results from these calculations are presented in Figure 11 where the excess pore pressure has been plotted as a function of time. The excess pore pressure decreases rapidly with time after completion of thawing, especially close to the pervious stratum. For example, at the depth of 2.4 ft below the ground surface, the excess pore pressure 580 hr after the initiation of the thawing is about 30 percent of the excess pore pressure after 530 hr of thawing.

It can be seen from Figure 11 that the dissipation of excess pore pressure due to the sudden lowering of water table after completion of thawing is considerably faster than that before complete thawing of the soil. Therefore, it is expected that the soil will regain its initial strength in a relatively short time once the subgrade soil is completely thawed. However, it should be noted that the dissipation of excess pore pressures is affected by the location of the pervious stratum which governs the stationary groundwater table. The time required for dissipation of excess pore pressures will increase rapidly with increasing distance of the pervious layer from the ground surface. The reason for the relatively long time required for dissipation of pore pressure at the depth of 0.4 ft below the ground surface is the location of the pervious layer. This layer is assumed to be located 3 ft below the ground surface.

SUMMARY

Methods have been developed by which excess pore pressures which develop during thawing of subgrade soils can be calculated. These methods are based on the premise that the rate of thawing and rate of liberation of excess pore water decrease with increasing thawing depth and the flow rate remains constant. The thawing rate can be calculated from the general differential equation which governs the one-dimensional unsteady heat flow. The dissipation of the resulting excess pore pressures can be calculated by Darcy's law. The use of these methods has been demonstrated by three examples.

It has been shown that the excess pore pressures which develop during thawing may be very high and that certain time periods exist, usually at the beginning of the thawing period, during which the subgrade is in a quick condition. When this occurs, the pore pressure is equal to the total overburden pressure and the resulting effective stress in soil approaches zero. Therefore, the bearing capacity of the subgrade may be very low during the spring months at the beginning of the thawing period. It has been shown that the excess pore pressures which develop in the subgrade during thawing decrease rapidly with increasing thickness of the base course. This indicates that the stability of a road may be increased considerably during thawing by the presence of a pervious base course.

The dissipation of excess pore pressures after completion of the thawing process has also been investigated. There is an increase in pore pressure (in addition to the excess pore pressure created during thawing) due to the sudden lowering of the temporarily perched groundwater table to the original groundwater table. The dissipation of these pore pressures can be calculated by the Terzaghi consolidation theory. The pore pressures decrease rapidly with time for those stratum located close to a pervious layer, and the soil will regain its initial strength within a relatively short time once the subgrade soil is completely thawed.

REFERENCES

1. Beskow, G. Tjalbildningen och Tjallyftningen (Soil Freezing and Frost Heaving, with Special Reference to Highways and Railroads). Statens Väginstitut, Meddelande 48, Sveriges Geologiska Undersökning, Ser. C., No. 375, Stockholm, 1935.
2. Beskow, G. Soil Freezing and Frost Heaving with Special Application to Roads and Railroads. Swedish Geological Soc., Ser. C, No. 375, 26th Yearbook, No. 3, 1935; with a special supplement for English translation of progress from 1935 to 1946. (Translated by J. O. Osterberg). Evanston, Ill., Northwestern Univ. Tech. Inst., Nov. 1947.
3. Broms, B. B. Bearing Capacity of Flexible Pavements Subject to Frost Action. Highway Research Record No. 39, pp. 166-180, 1963.
4. Broms, B. B., and Yao, L. Y. C. Shear Strength of a Soil After Freezing and Thawing. Jour. Soil Mech. and Found. Div., Proc. ASCE, Vol. 90, No. SM4, July 1964.
5. Report on Frost Investigation, 1944-1945. U. S. Army Corps of Engineers, New England Div., 1947.
6. Addendum No. 1., 1945-1947, Report on Frost Investigation, 1944-45. U. S. Army Corps of Engineers, New England Div., Frost Effects Lab., 1949.
7. Gibson, R. E., and Lumb, P. Numerical Solution of Some Problems in Consolidation of Clay. Proc. Inst. of Civil Eng., Vol. 2, Pt. 1, pp. 182-198, 1953.
8. Haley, J. F., and Capler, C. W. Cold Room Studies of Frost Action in Soil. Highway Research Board Spec. Rept. No. 2, pp. 246-267, 1952.
9. Jumikis, A. R. Suction Force in Soils Upon Freezing. Proc. ASCE, Vol. 80, Sep. No. 445, 1954.
10. Jumikis, A. R. The Frost Penetration Problem in Highway Engineering. New Brunswick, N. J., Rutgers Univ. Press, 1955.
11. Leonards, G. A. Foundation Engineering. New York, McGraw-Hill, 1962.

12. Linell, K. A., and Haley, J. F. Investigation of the Effect of Frost Action on Pavement-Supporting Capacity. Highway Research Board Spec. Rept. No. 2, pp. 295-325, 1952.
13. Meyerhof, G. G. The Ultimate Bearing Capacity of Foundation. Geotechnique, Vol. 2, p. 301, 1951.
14. Load-Carrying Capacity of Frost-Affected Roads. Highway Research Board Bull. 96, 1955. 23 pp.
15. Penner, E. The Mechanism of Frost Heaving in Soil. Highway Research Board Bull. 225, pp. 1-22, 1959.
16. Prandtl, L. Uber die Harte Plastischen Korper. Nachr. Ges. Wiss. Gottingen, 1920.
17. Skempton, A. W., and Bishop, A. W. Soils. In Building Materials, Their Elasticity and Inelasticity (M. Reiner, ed.), Chap. 10. Amsterdam, North-Holland Publishing Co., 1954.
18. Taber, S. Frost Heaving. Journal of Geology, Vol. 37, No. 5, pp. 428-461, July-August 1929.
19. Taber, S. The Mechanics of Frost Heaving. Journal of Geology, Vol. 38, No. 4, pp. 303-317, May-June 1930.
20. Terzaghi, K. Theoretical Soil Mechanics. New York, John Wiley and Sons, 1943.

Appendix

NOTATIONS

A = area (sq ft);

$\bar{A}_f$ = pore pressure coefficient;

a = thickness of pavement, ft;

c = specific heat;

c_u = apparent cohesion determined by undrained triaxial or direct shear tests (psf);

c' = apparent cohesion with respect to effective stresses determined from consolidated-undrained triaxial or direct shear tests (psf);

G_S = specific gravity of solids;

H = equivalent thickness (ft) (Eq. 25);

H_a = location below ground surface of permanent groundwater table (ft);

H_1 = thickness of base course (ft);

h = length of flow path (ft);

i = hydraulic gradient;

K_o = coefficient of lateral earth pressure at rest;

K, K_1 = coefficient of thermal conductivity (Btu/ft-hr-°F) (Eq. 7b);

k = permeability of soils (ft/hr);

m, m_1 = $\sqrt{\frac{2K_1(T_S - T_f)}{Q_L \gamma_w n}}$ (Eq. 8c);

n = porosity;

N_c = bearing capacity factor;

p_o = initial total pressure (psf);

$\bar{p}_o$ = initial effective pressure (psf);

p_1 = major total principal stress (psf);

p_3 = minor total principal stress (psf);

q_{ult}^{net} = net ultimate bearing capacity, (psf);

Q = excess melted water (cu ft);

Q_L = latent heat of fusion (Btu/lb);

S_r = degree of saturation (%);

t = elapsed time from beginning of thawing period (hr);

T = temperature at time t and depth Z (°F);

T_s = surface temperature (°F);

T_f = freezing temperature (°F);

u = total pore pressure (psf);

u_o = static or initial pore pressure (psf);

u_{excess} = excess pore pressure (psf);

V = total volume (cu ft);

v = flow velocity (ft/hr);

w = moisture content of frozen soil (%);

w_o = moisture content of thawed soil (%);

Z, Z_1, Z_2 = depth (ft);

Z_{cr} = critical depth (ft) (Eq. 18);

Z_o = depth of thawing (ft) (Eq. 8a);

φ' = apparent angle of internal friction with respect to effective stresses measured by consolidated-undrained triaxial or direct shear tests (deg);

γ_p = unit weight of pavement material (pcf);

γ_{sat} = saturated unit weight of soil (pcf);

γ_{sub} = submerged unit weight of soil (pcf);

γ_w = unit weight of water (pcf);

α = thermal diffusity (sq ft/hr); and

ρ = density of material (pcf).